Shedding light on Dark Matter Using Extended Higgs Sectors

Juhi Dutta

National Taiwan University, Taipei, Taiwan

The 16th Particle Physics Phenomenology Workshop

based on

Eur.Phys.J.C 84 (2024) 9, 926, Eur.Phys.J.Plus 140 (2025) 1, 87 , Eur.Phys.J.C 86 (2026) 4, 384

with G. Moorgat-Pick, J.Lahiri, C.Li, M.Schreiber, S.F.Tabira, J.A.Ziegler

June 17, 2026

The Standard Model of Particle Physics

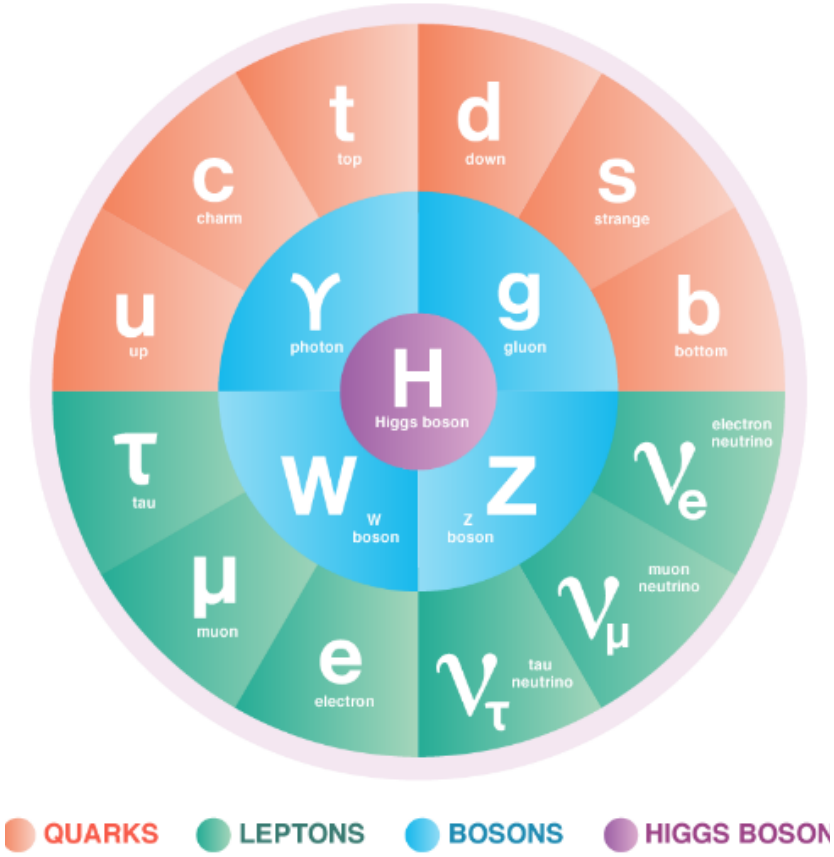

The Standard Model of Particle Physics, FERMILAB

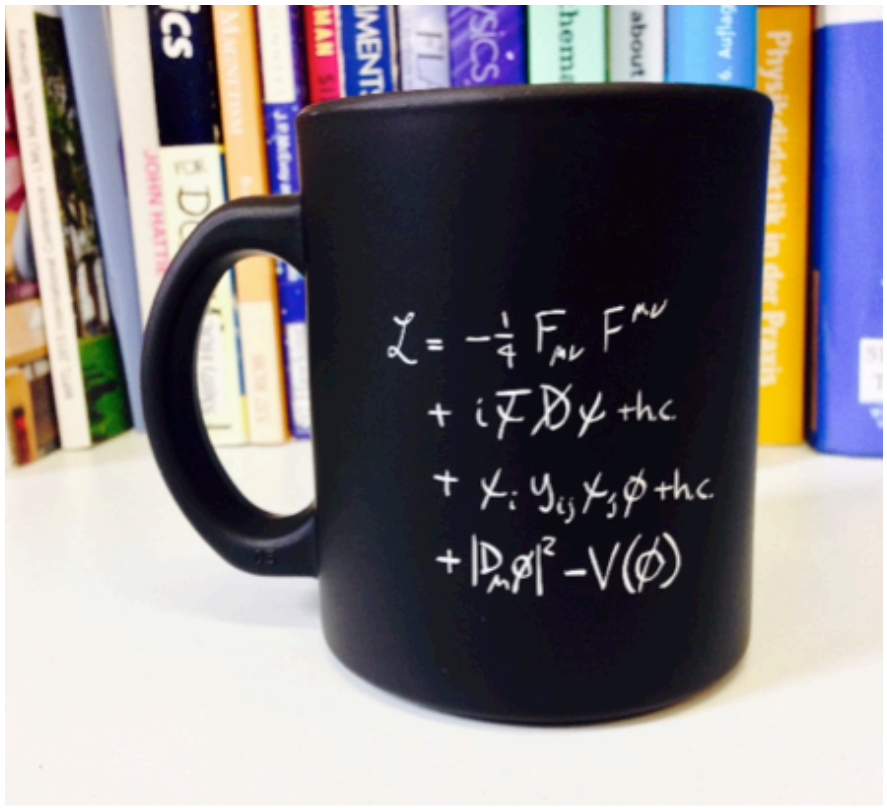

CERN

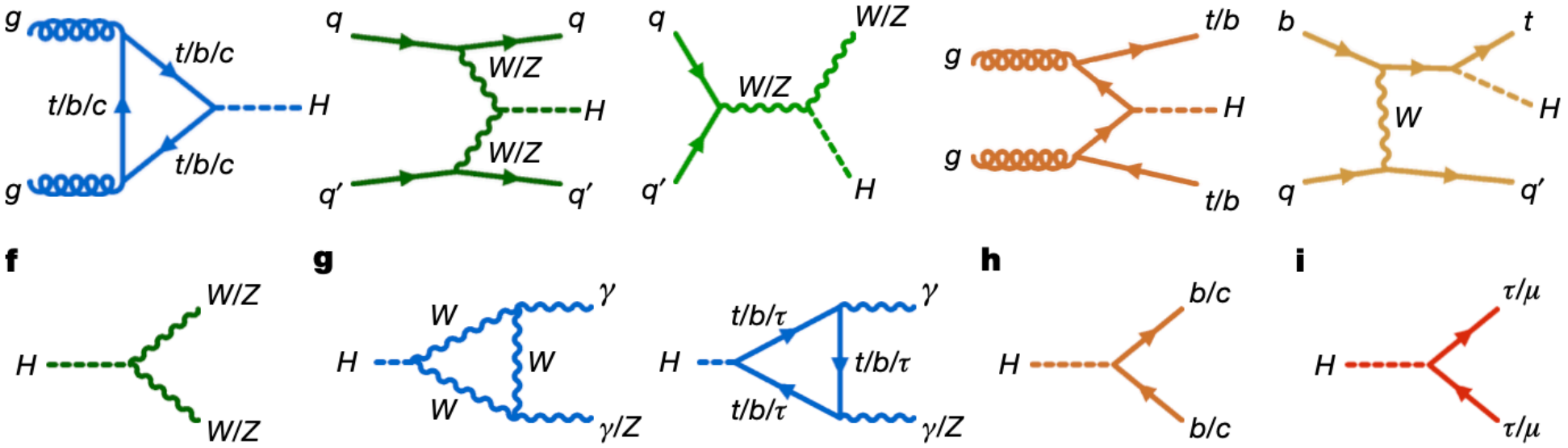

No. of. events

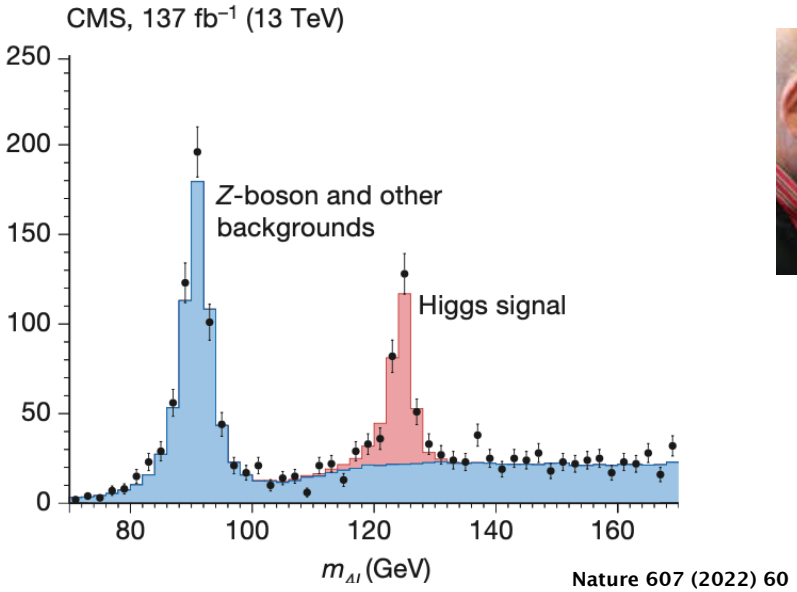

Nature 607 (2022) 60

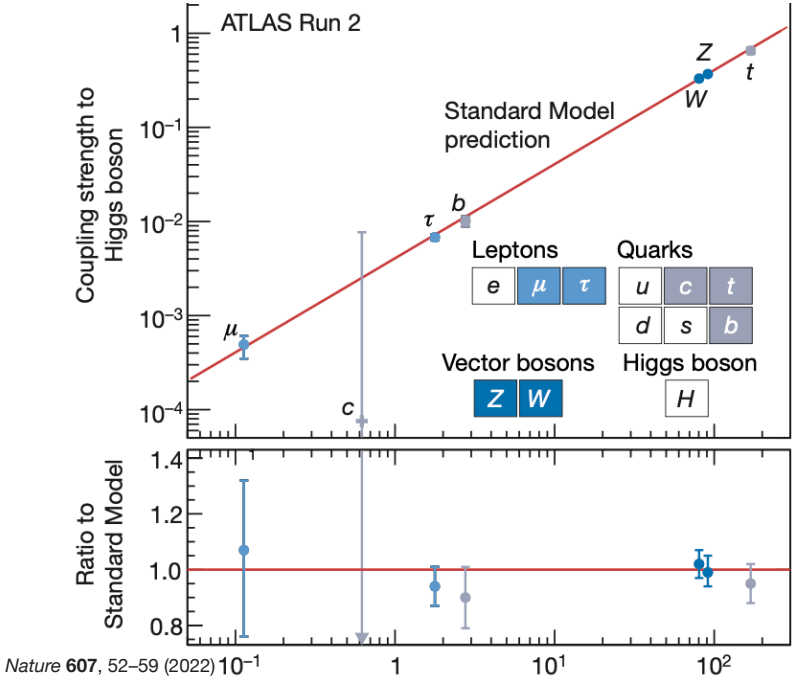

Nature **607**, 52–59 (2022)

Open Questions..

- Gauge hierarchy problem
- Dark Matter
- Dark Energy
- Non-zero neutrino masses
- Matter-antimatter asymmetry
- Strong CP-problem
- Gravity

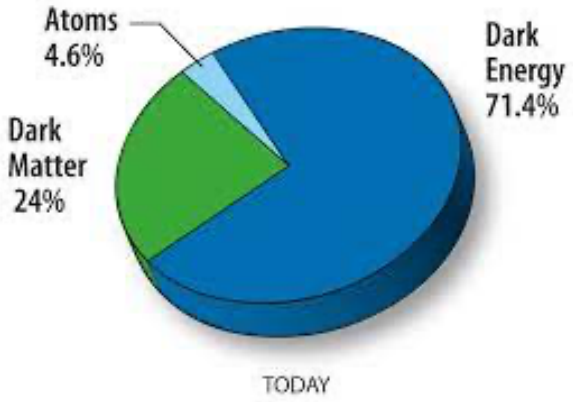

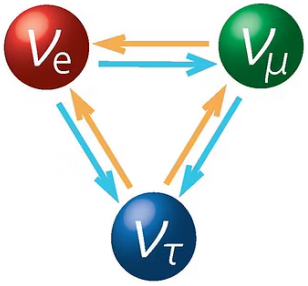

Synergy of Higgs to New Physics?

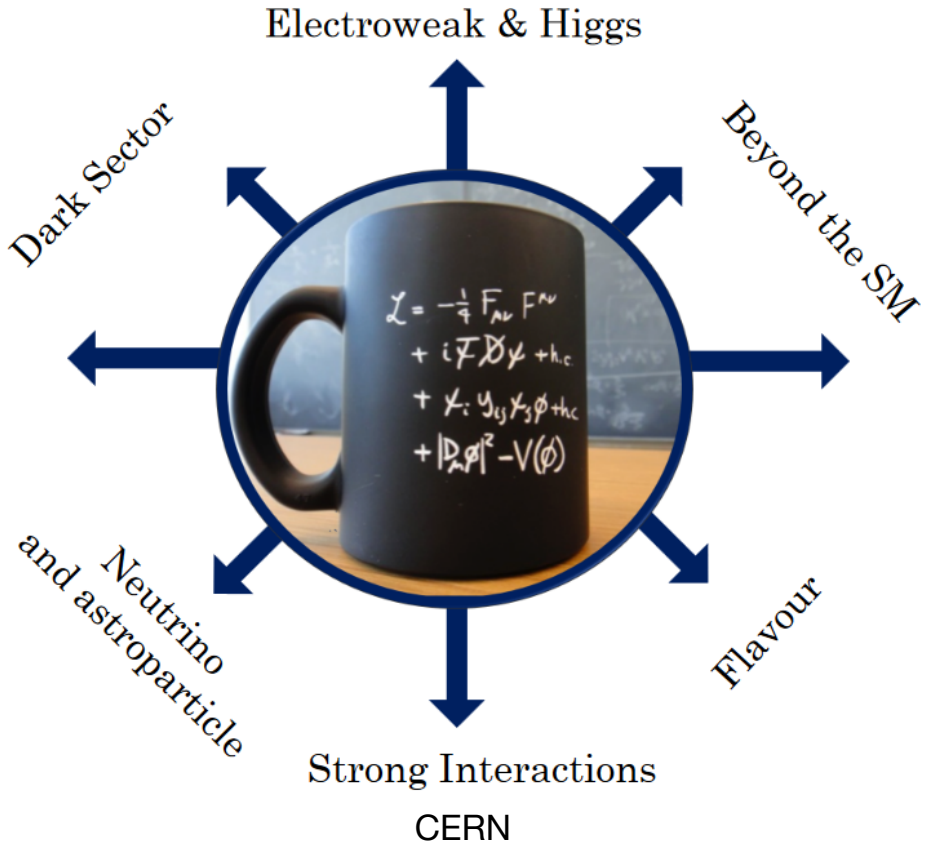

Dark Matter

Evidences

Rotational velocity of Galaxies

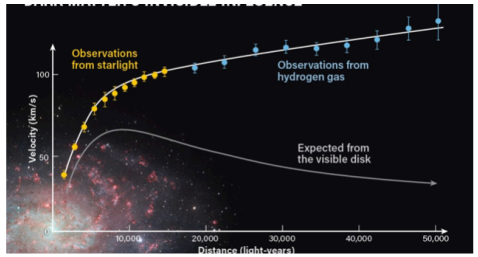

Bullet Cluster

Gravitational Lensing

CMB

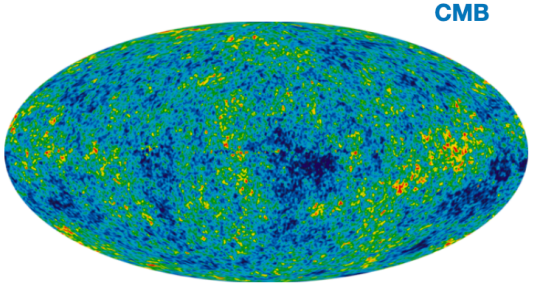

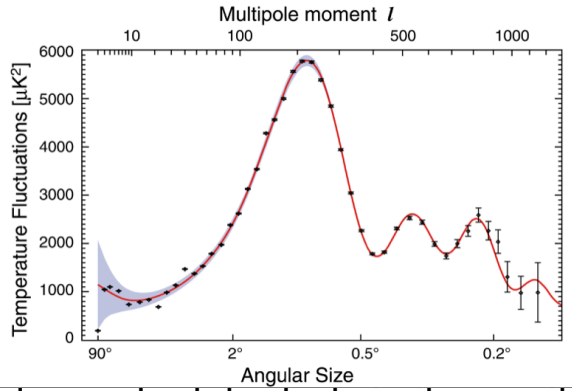

BAO

What do we know?

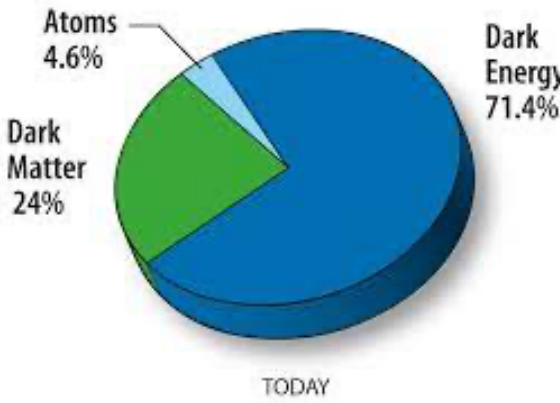

$$\Omega_{\rm DM} h^2 = 0.12 \pm 0.001$$

- DM must be electrically neutral as only detected via its gravitational interactions.
- Stable at least until the lifetime of the Universe.
- Mass and nature unknown!

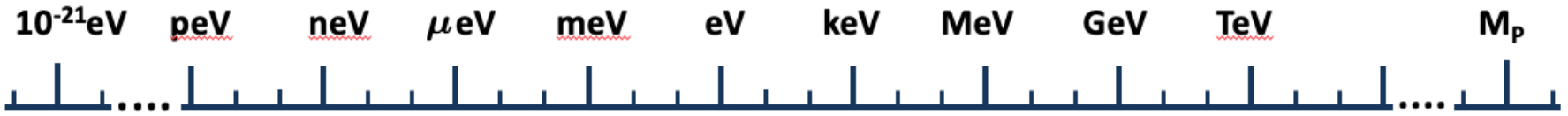

Dark Matter: Detection

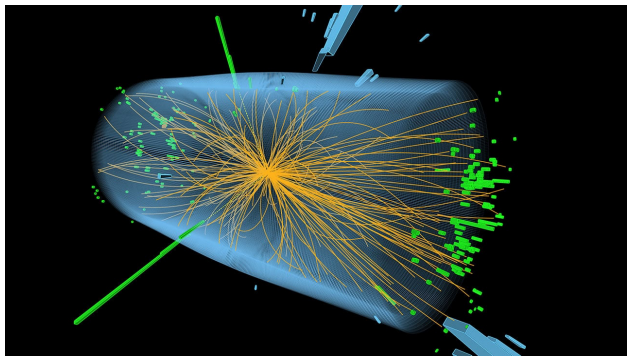

(HL)-LHC, FCC,
ILC, Muon Colliders…

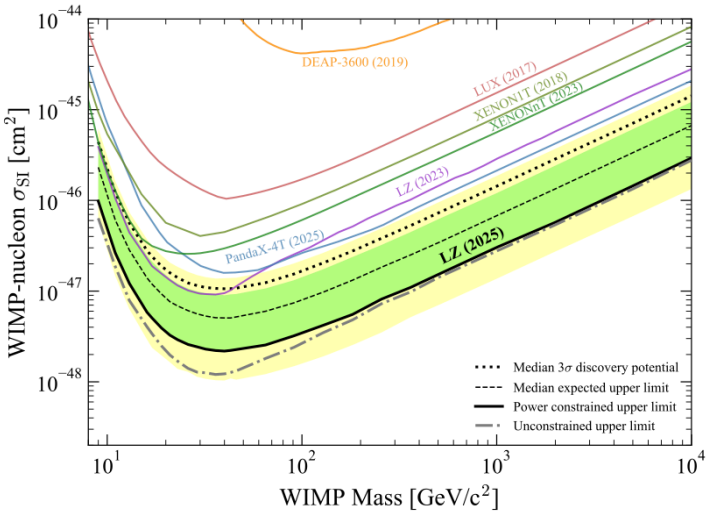

LZ, Xenon I(n) T, Panda X, Darwin..

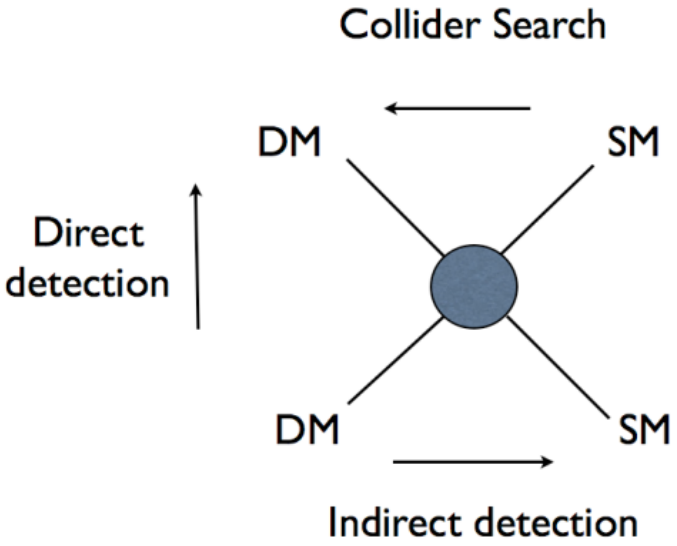

Fermi-LAT

Looking for Dark Matter

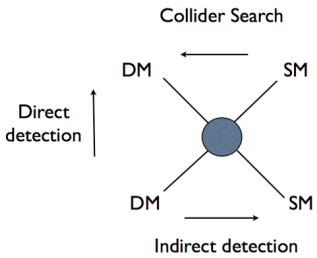

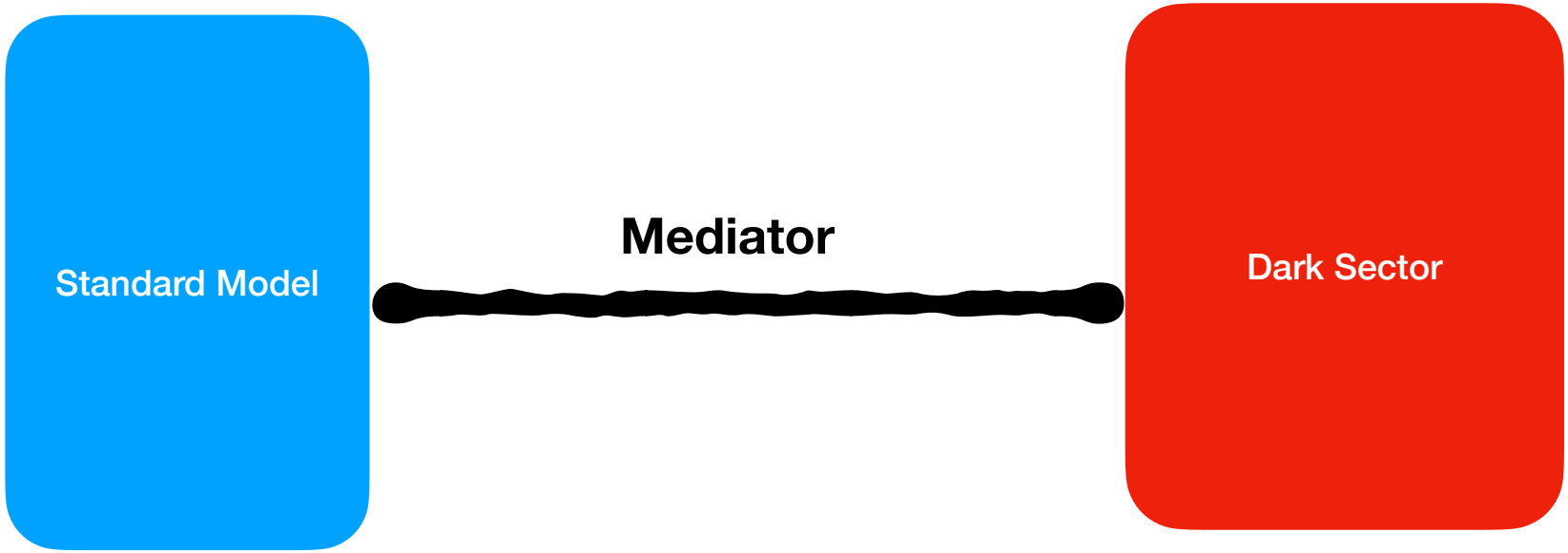

Higgs as a portal to the Dark Sector

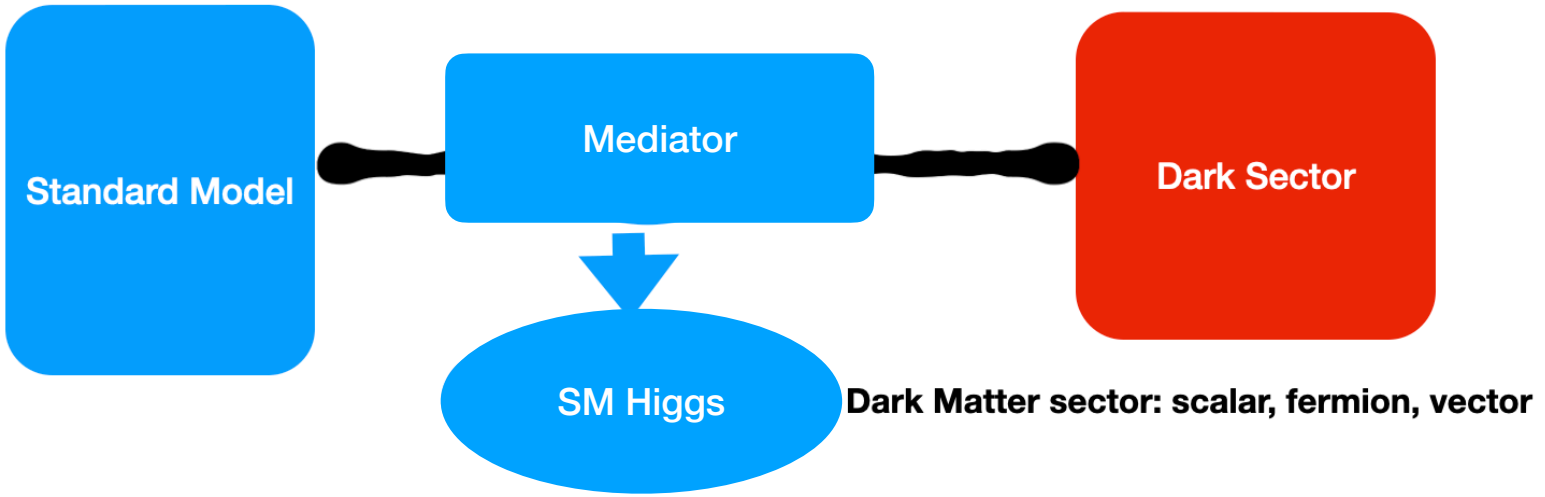

The SM Higgs Portal

- Scalar singlets under the SM gauge group $\Longrightarrow$ potential dark matter candidates.

Barger, et.al Phys.Rev.D79:015018,2009

- It communicates to the SM via the 125 GeV Higgs as the portal to the dark sector.

- Stringently constrained from dark matter direct detection data.

Higgs(es) as portals to the Dark Sector

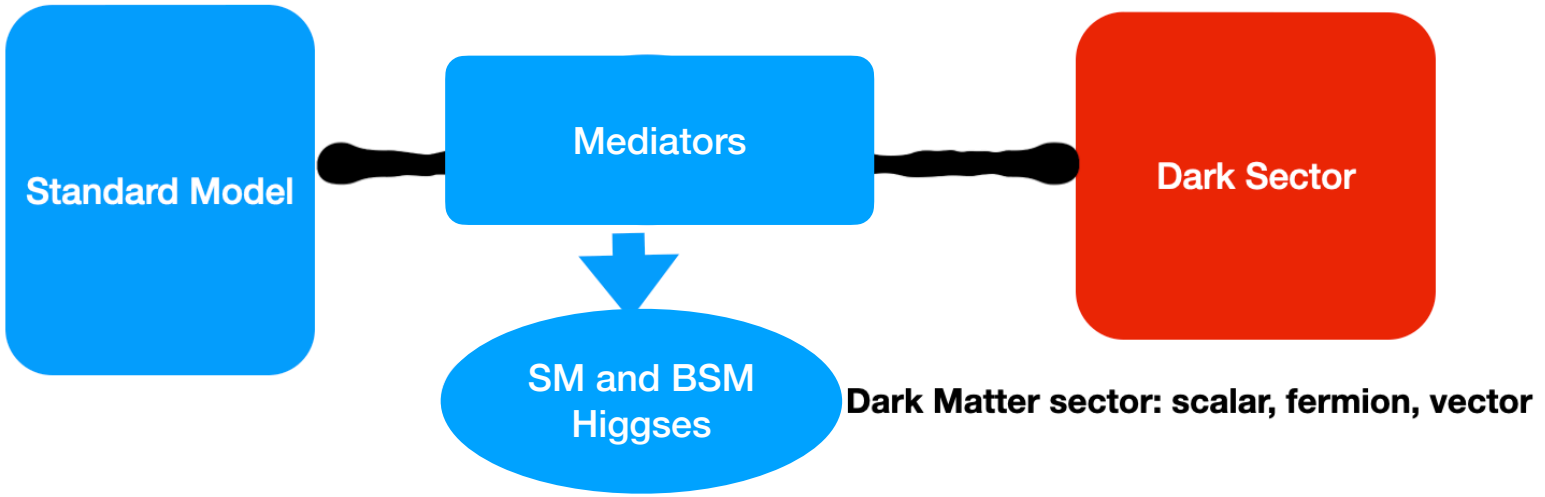

- Presence of additional portals to dark matter via extra Higgses as in singlet extended multi-Higgs models relaxes direct detection constraints with prospects for collider signals.

Extended Higgs Sectors

Dark Matter

Higgs Phenomenology

Scalar excesses, e.g, "~95 GeV" excess

Inflation

Baryogenesis

Leptogenesis

Gravitational Waves

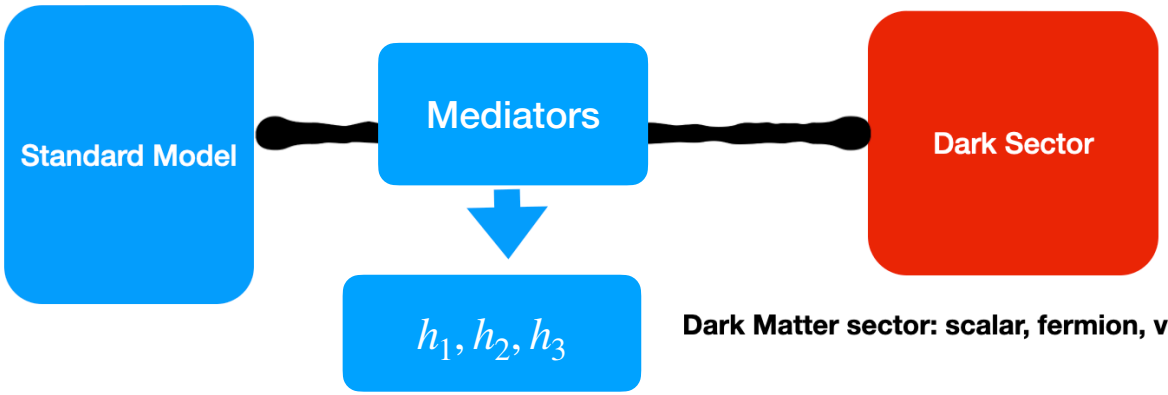

Dark Matter sector: scalar, fermion, vector

Eg. in
2HDM + complex singlet scalar (2HDMS) with DM stabilized by a Z_2' symmetry.

Baum, et.al, *JHEP*12(2018)044

Dutta et.al, Eur.Phys.J.Plus 140 (2025) 1, 87, 2504.14529,

Eur.Phys.J.C 84 (2024) 9, 926, ongoing works.

S.Heinemeyer et.al, Phys. Rev. D 106 (2022), no. 7 075003

Matlis et.al, JCAP 07 (2024) 007

Biekotter,et.al 2509.01682, JHEP 10 (2022) 126

Drozd et.al JHEP11 (2014) 105, Dey et.al JHEP 09 (2019) 004

Extended Higgs Portal Models:
2HDM + complex singlet scalar (2HDMS)

- Consider a softly broken Z_2 (to avoid FCNC) symmetric Type II 2HDM augmented with a complex scalar singlet S, with the imaginary component stabilized under Z_2'.

- Depending on the singlet vev v_S, the model can accommodate single or multicomponent dark matter candidates.

- The scalar potential is: $V_{2HDMS} = V_{2HDM} + V_S$,

Model	u_R^i	d_R^i	e_R^i
Type I	Φ_2	Φ_2	Φ_2
Type II	Φ_2	Φ_1	Φ_1
Lepton-specific	Φ_2	Φ_2	Φ_1
Flipped	Φ_2	Φ_1	Φ_2

$$\Phi_i = \begin{pmatrix} \phi_i^{\pm} \\ \frac{1}{\sqrt{2}}(v_i + h_i + ia_i) \end{pmatrix}, \quad i = 1, 2,$$

$$S = \frac{1}{\sqrt{2}}(v_S + h_S + ia_S)$$

$$V_{2HDM} = m_{11}^2\Phi_1^\dagger\Phi_1 + m_{22}^2\Phi_2^\dagger\Phi_2 - (m_{12}^2\Phi_1^\dagger\Phi_2 + h.c) + \frac{\lambda_1}{2}(\Phi_1^\dagger\Phi_1)^2 + \frac{\lambda_2}{2}(\Phi_2^\dagger\Phi_2)^2 + \lambda_3(\Phi_1^\dagger\Phi_1)(\Phi_2^\dagger\Phi_2) + \frac{\lambda_4}{2}(\Phi_1^\dagger\Phi_2)(\Phi_2^\dagger\Phi_1) + \frac{\lambda_5}{2}(\Phi_1^\dagger\Phi_2)^2 + h.c,$$

$$V_S = m_S^2(S^\dagger S) + \frac{m_S^{2'}}{2}(S^2 + h.c) + \frac{\lambda_1''}{24}(S^4 + h.c) + \frac{\lambda_2''}{6}(S^2(S^\dagger S) + h.c) + \frac{\lambda_3''}{4}(S^\dagger S)^4 + \lambda_1' S^\dagger S\Phi_1^\dagger\Phi_1 + \lambda_2' S^\dagger S\Phi_2^\dagger\Phi_2 + S^2(\lambda_4'\Phi_1^\dagger\Phi_1 + \lambda_5'\Phi_2^\dagger\Phi_2) + h.c.$$

Baum, et.al, *JHEP*12(2018)044

Key Points

Particle content:

$$h_1, h_2, h_3, A, H^{\pm}, A_S$$

Scalar Mediators **DM**

Dark Matter mass:

$$m^2_{A_S} = \frac{\partial^2 V}{\partial A_S^\dagger \partial A_S}\Big|_{\substack{\Phi_1=\langle\Phi_1\rangle \\ \Phi_2=\langle\Phi_2\rangle \\ S=\langle S\rangle}}$$

$$= -(2m'^2_S + v_S^2(\frac{\lambda''_1}{3} + \frac{\lambda''_2}{3}) + 2(\lambda'_4 v_1^2 + \lambda'_5 v_2^2))$$

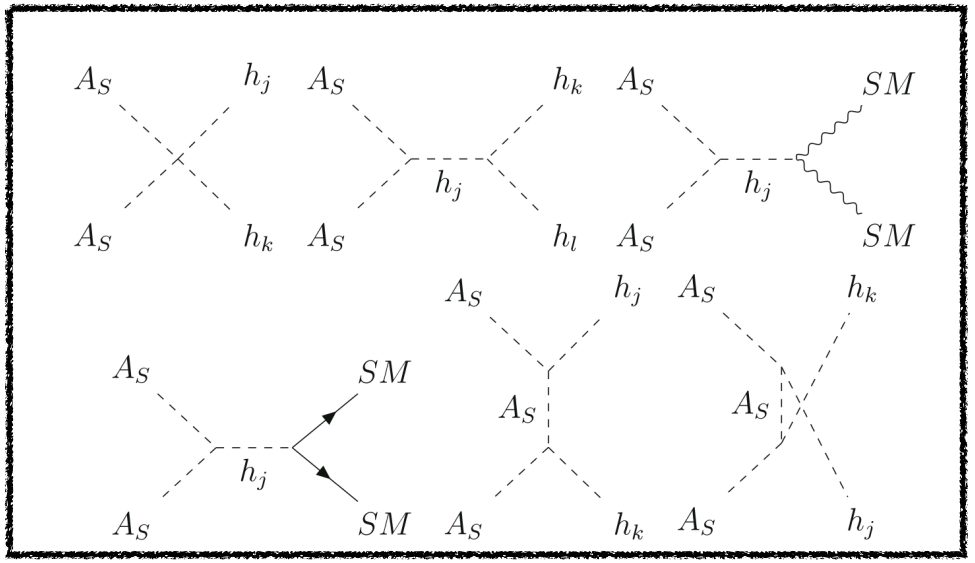

Free parameters:

$$m_{h_1}, m_{h_2}, m_{h_3}, m_A, m_{H^\pm}, m_{A_S}, \tan\beta, v_S, \tilde{\mu}^2, \alpha_1, \alpha_2, \alpha_3$$
$$\lambda'_{14} = \lambda'_1 - 2\lambda'_4, \lambda'_{25} = \lambda'_2 - 2\lambda'_5, \lambda''_{13} = \lambda''_1 - \lambda''_3,$$

$$R = \begin{pmatrix} c_{\alpha_1}c_{\alpha_2} & s_{\alpha_1}c_{\alpha_2} & s_{\alpha_2} \\ -s_{\alpha_1}c_{\alpha_3} - c_{\alpha_1}s_{\alpha_2}s_{\alpha_3} & c_{\alpha_1}c_{\alpha_3} - s_{\alpha_1}s_{\alpha_2}s_{\alpha_3} & c_{\alpha_2}s_{\alpha_3} \\ s_{\alpha_1}s_{\alpha_3} - c_{\alpha_1}s_{\alpha_2}c_{\alpha_3} & -c_{\alpha_1}s_{\alpha_3} - s_{\alpha_1}s_{\alpha_2}c_{\alpha_3} & c_{\alpha_2}c_{\alpha_3} \end{pmatrix},$$

Connection to colliders via invisible decays of SM and BSM Higgs bosons.

Trilinear and Quartic Couplings of DM to Higgs Bosons:

$$\frac{\lambda_{h_j A_S A_S}}{v} = -i[\lambda'_{14}c_\beta R_{j1} + \lambda'_{25}s_\beta R_{j2} - \frac{v_S}{2v}\lambda''_{13}R_{j3}]$$
$$\lambda_{h_j h_k A_S A_S} = -i[\lambda'_{14}R_{j1}R_{k1} + \lambda'_{25}R_{j2}R_{k2} - \frac{1}{2}\lambda''_{13}R_{j3}R_{k3}],$$

Dutta et.al, *Eur.Phys.J.C 86 (2026) 4, 384*

Extended Higgs sectors as portals for pseudoscalar Dark Matter

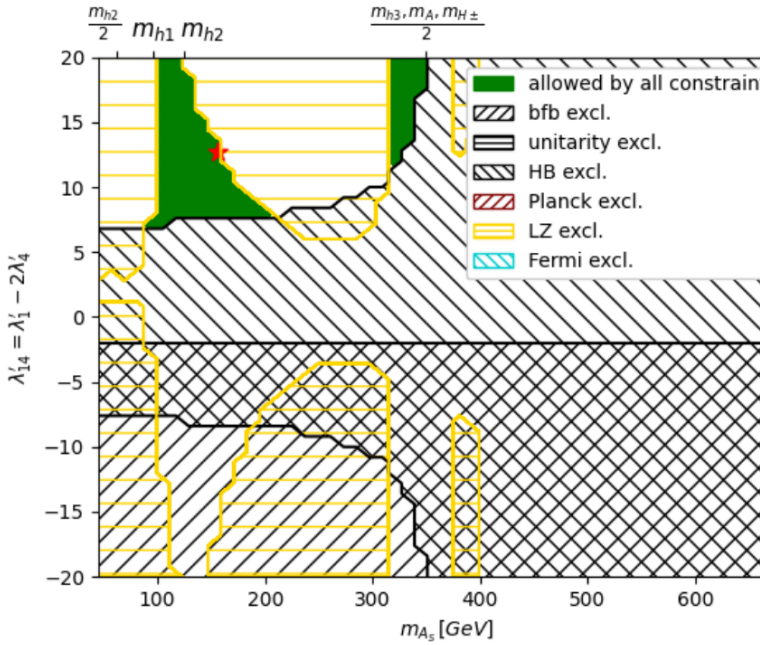

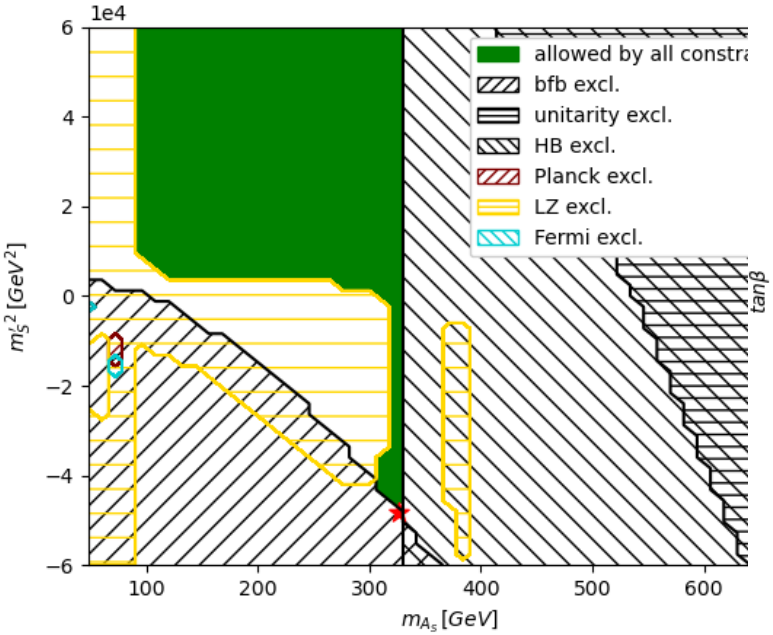

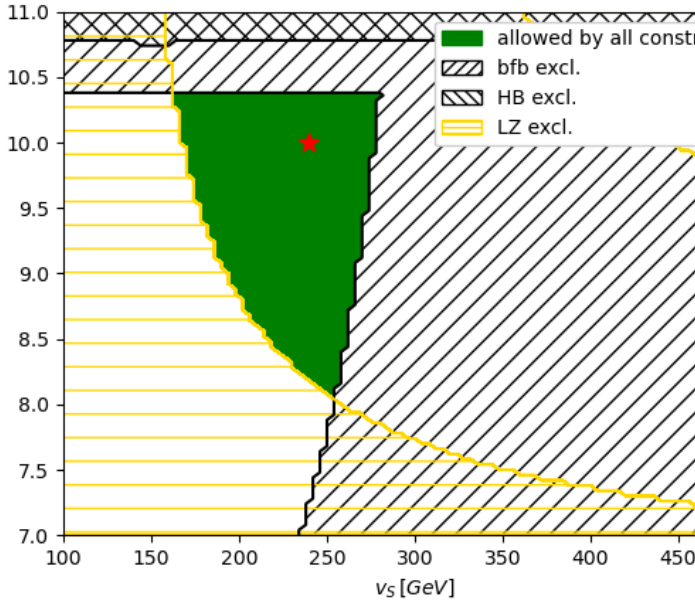

Unitarity, BFB,
B physics constraints
Higgs Mass Bounds
SM Higgs Signal Strengths

Relic Density
SI cross-section
ID cross-section

Allowed Parameter Space subject to theory and experimental constraints.

Representative Benchmarks

with 95 GeV light scalar **without 95 GeV light scalar**

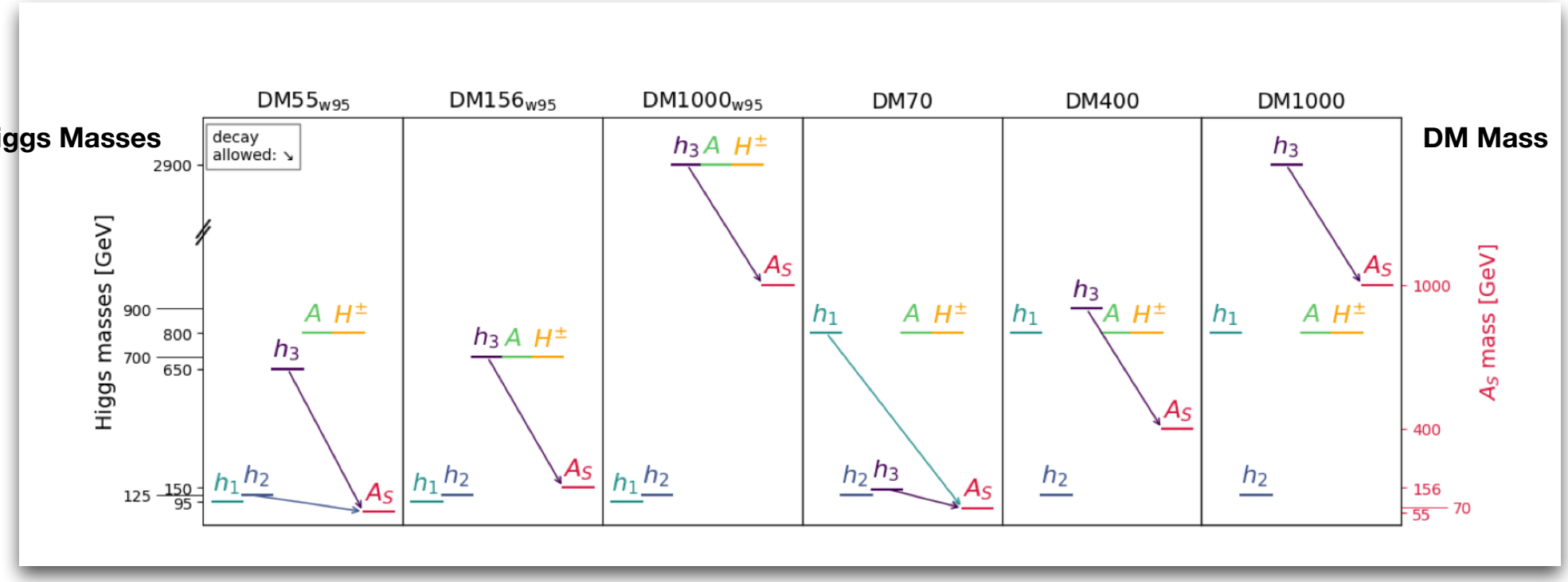

Low mass **Intermediate mass** **High Mass** **Low mass** **Intermediate mass** **High Mass**

Connection to colliders and benchmarks

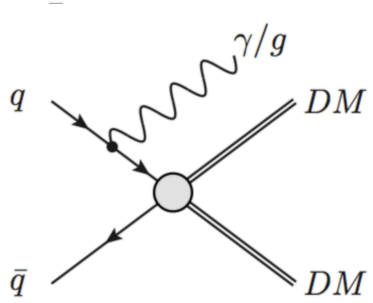

- DM invisible to colliders.
- Typical signals: SM particles + Missing energy, eg. Mono-X + MET

	m_{A_S} (GeV)	$\tan\beta$	Ωh^2	$BR(h_1 \to A_S A_S)$	$BR(h_2 \to A_S A_S)$	$BR(h_3 \to A_S A_S)$
DM55$_{\mathbf{w95}}$	55	2	0.11	-	0.0199	$3.81 \cdot 10^{-9}$
DM156$_{\mathbf{w95}}$	156	6.6	$1.61 \cdot 10^{-4}$	-	-	0.692
DM1000$_{\mathbf{w95}}$	1000	5	0.111	-	-	0.0360
DM70	70	1.37	0.113	$1.80 \cdot 10^{-4}$	-	0.999
DM400	400	2.13	0.106	-	-	0.822
DM1000	1000	1.34	0.117	-	-	0.00514

- Benchmarks chosen with thermal relic and underabundant cases satisfying all theoretical and experimental constraints.
- Potential signals at high luminosity LHC, e+e- colliders as well as muon colliders.

Present and future colliders

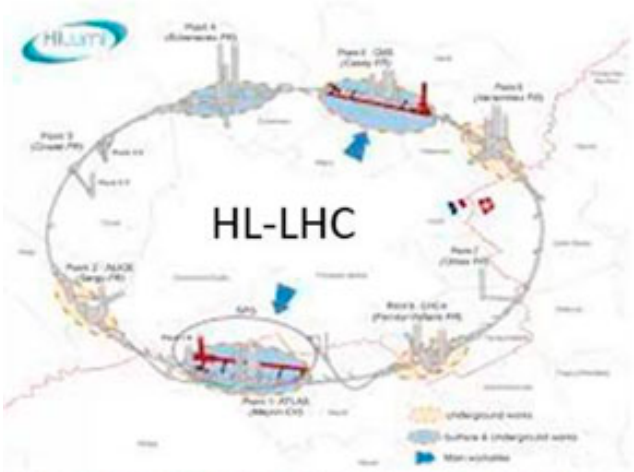

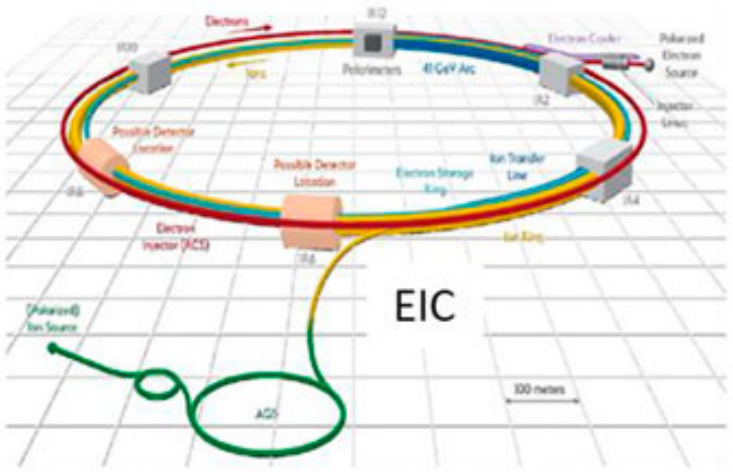

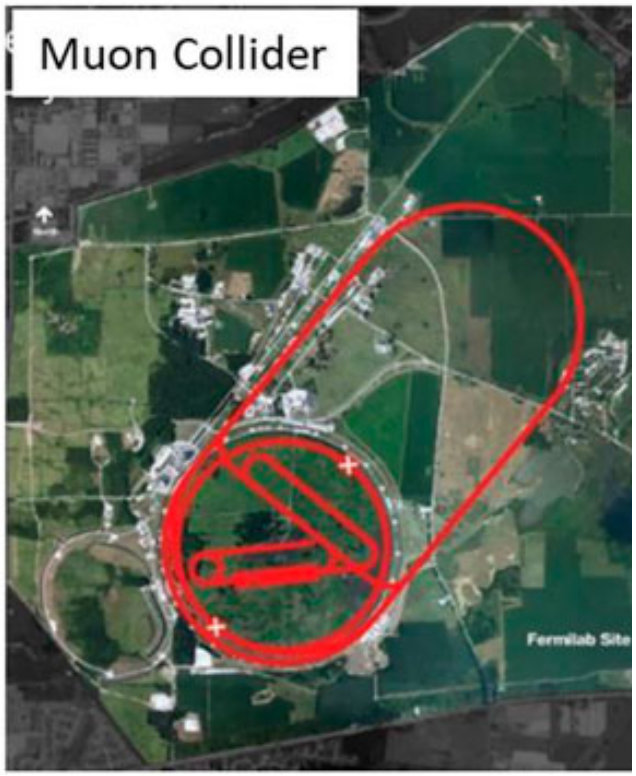

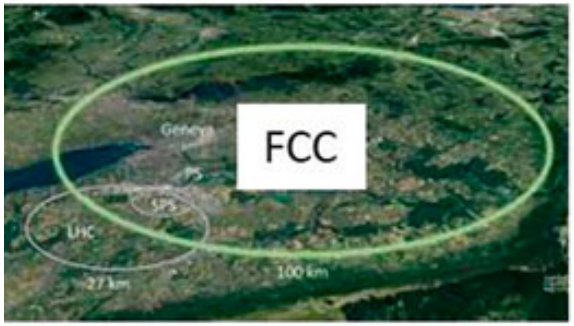

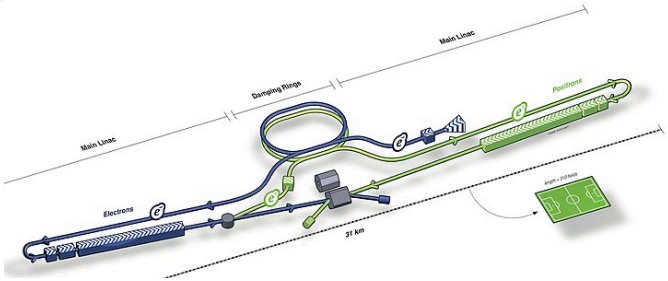

ILC

Signals at HL-LHC

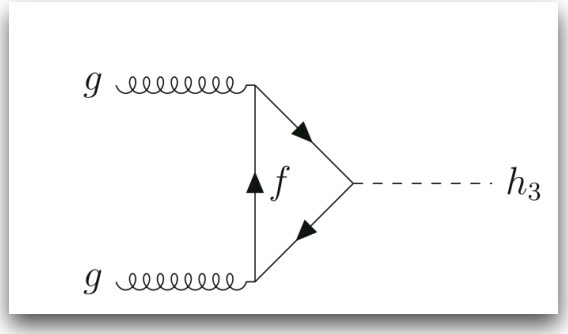

Gluon Fusion (GGF)

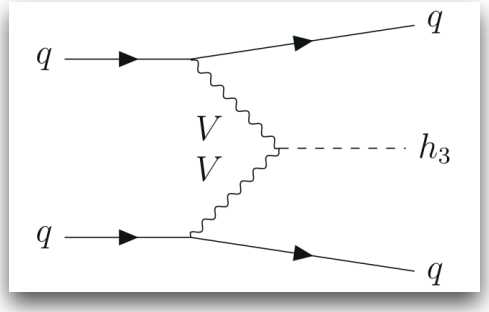

Vector Boson Fusion (VBF)

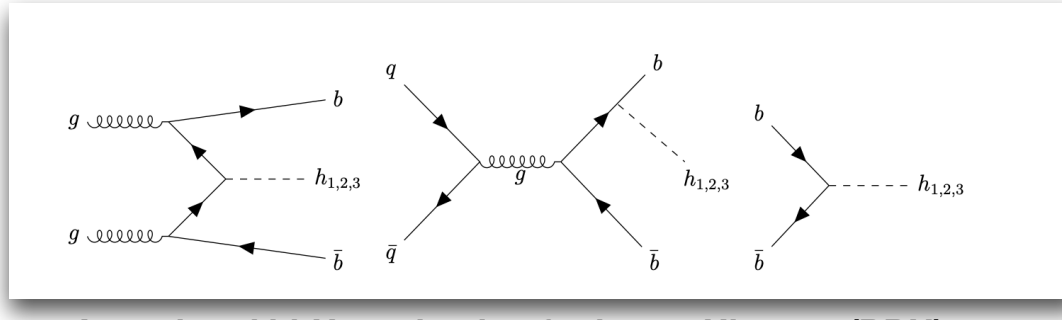

Associated bbH production for heavy Higgses (BBH)

Process	Production cross-section (fb) at $\sqrt{s} = 14$ TeV		
	DM55$_{w95}$	**DM156$_{w95}$**	**DM70**
GGF ($h_2 \to A_S A_S$)	533.9	–	19.29×10^3
GGF ($h_3 \to A_S A_S$)	–	0.015	–
VBF ($h_2 \to A_S A_S$)	54.33	–	2.72×10^3
VBF ($h_3 \to A_S A_S$)	–	0.134	0.0022
BBH ($(b\bar{b}h_2 \to A_S A_S)$)	21.6	–	0.137
BBH ($(b\bar{b}h_3 \to A_S A_S)$)	–	47.24	–

Production cross-sections of different channels at HL-LHC.

Gluon Fusion

Mono-jet + MET signal:

- **C1**: The final state consists of up to four jets with $p_T > 30$ GeV and $|\eta| < 2.8$.
- **C2**: We demand a large $\not{E}_T > 250$ GeV.
- **C3**: The hardest leading jet has $p_T > 250$ GeV with $|\eta| < 2.4$.
- **C4**: We demand $\Delta\Phi(j, \not{E}_T) > 0.4$ for all jets and $\Delta\Phi(j, \not{E}_T) > 0.6$ for the leading jet.
- **C5**: A lepton-veto is imposed for electrons with $p_T > 20$ GeV and $|\eta| < 2.47$ and muons with $p_T > 10$ GeV and $|\eta| < 2.5$.

Benchmark	Significance
DM55$_{w95}$	0.30σ
DM70	0.55σ

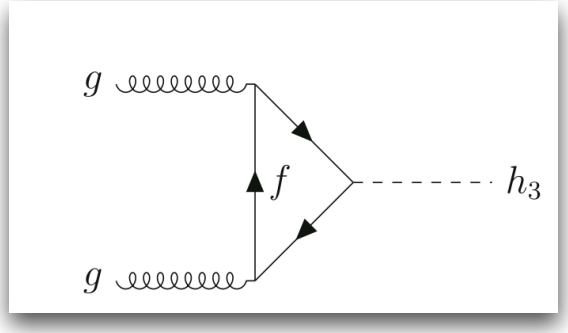

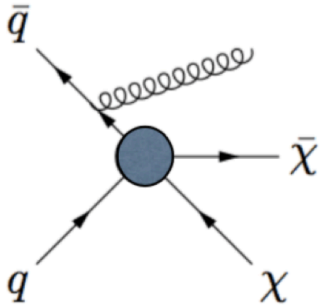

monojet +MET

ATLAS Collaboration, JHEP 01, 126 (2018)

Vector Boson Fusion

2 j + MET final state:

- **D1**: The final state consists of at least two jets with $p_T(j_1) > 80$ and $p_T(j_2) > 40$ GeV and $\Delta\Phi(j_i, \not{E}_T) > 0.5$.
- **D2**: We demand $\eta(j_1 j_2) < 0$ and $\Delta\Phi j_1 j_2 < 1.5$.
- **D3**: We demand $|\Delta\eta|_{jj} > 3.0$.
- **D4**: The invariant mass of the two forward jets is required to be large, i.e, $M_{jj} > 600$ GeV.
- **D5**: We demand $\not{E}_T > 200$ GeV.
- **D6**: Furthermore, a lepton veto is imposed for electrons with $p_T > 20$ GeV or muons with $p_T > 10$ GeV.

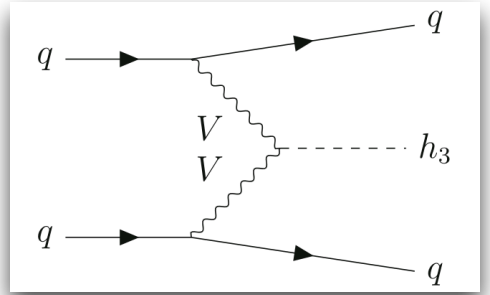

Benchmark	Significance
DM70	1.94σ

CMS Collaboration, Phys. Lett. B 793, 520–551 (2019)

Associated Higgs production

2 b + MET signal:

- **E1**: The final state consists of two b jets and no photons or leptons. We demand $\Delta R(b_1, b_2) > 0.4$, $p_T(b_1) > 150$ GeV and $p_T(b_2) > 100$ GeV.
- **E2**: We demand a large missing transverse momenta (MET) $\not{E}_T > 200$ GeV to reduce SM background.
- **E3**: We demand $M(b\bar{b}) > 200$ GeV to reduce SM background contributions.

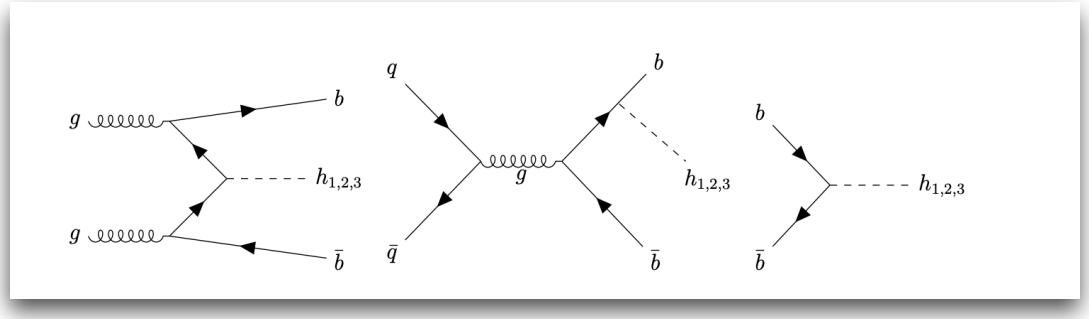

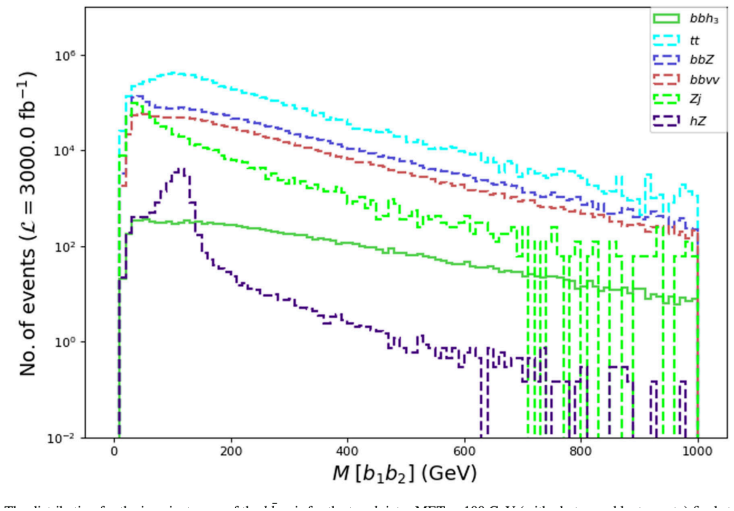

Benchmark	Cross-section after cuts (fb)
DM156$_{w95}$	0.357
SM Background	
$b\bar{b}Z$	18.3
$b\bar{b}\nu\bar{\nu}$	13.46
$t\bar{t}$	66.46
$Z + j$	2.04
$h\bar{Z}$	0.012
Total background	100.27

Benchmark	Significance
DM156$_{w95}$	1.95σ

Salient Points

- Signals: Mono-jet + Missing energy, Di-jet + Missing Energy, 2b jets + Missing energy
- Competitive reach from VBF and BBH for light DM benchmarks.
- Hints of new physics ~2σ by the end of high luminosity LHC at 14 TeV and 3000 fb^{-1}.
- Enhancement of cross-sections by a factor 100-1000 at Future Circular Collider (FCC-hh).

Process	Production cross-section (fb) at $\sqrt{s} = 100$ TeV		
	DM55$_{w95}$	**DM156$_{w95}$**	**DM70**
GGF ($h_2 \to A_S A_S$)	10.1×10^5	–	4.09×10^5
GGF ($h_3 \to A_S A_S$)	–	1.596	–
VBF ($h_2 \to A_S A_S$)	5.97×10^2	–	81.87
VBF ($h_3 \to A_S A_S$)	–	3.12	–
BBH ($h_2 \to A_S A_S$)	6.43×10^2	–	17.2×10^3
BBH ($h_3 \to A_S A_S$)	–	5.00	–

- Lepton colliders could play a crucial role here to uncover these scenarios with better precision and cleaner environment.

Signals at lepton colliders

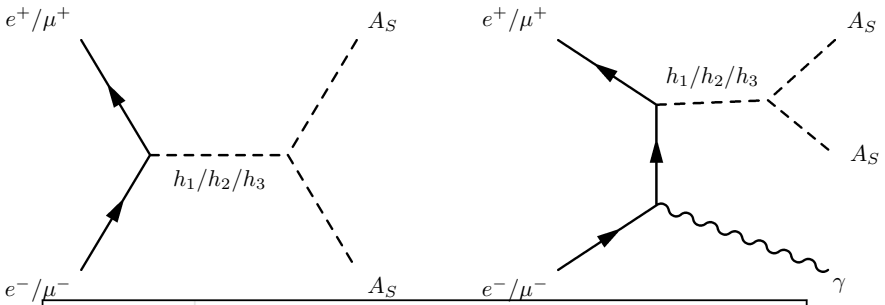

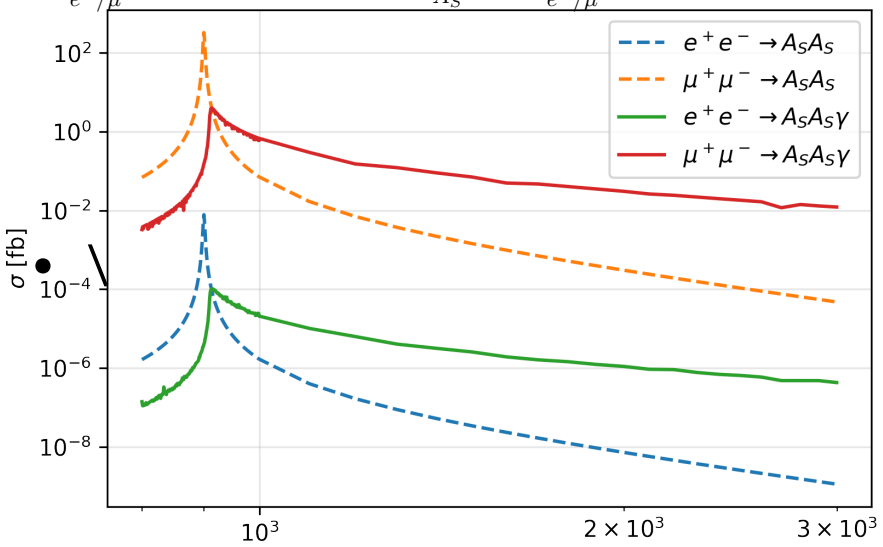

Mono γ+ Missing Energy

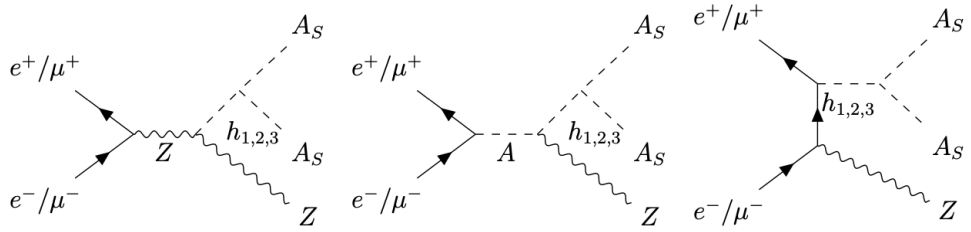

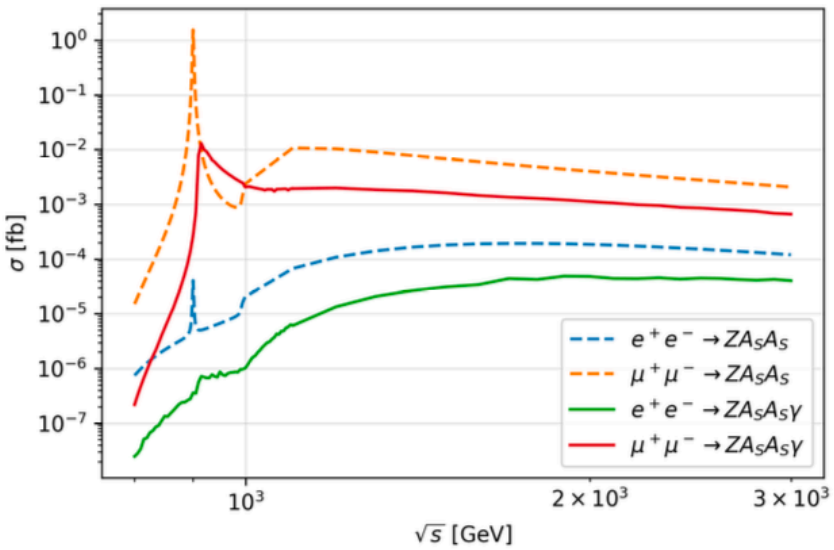

Mono-Z + Missing Energy

Significant enhancements near the higgs resonance region observed in muon colliders due to the muon Yukawa coupling $\Longrightarrow$ complementary searches to LHC.

Relevant processes at e+e- colliders

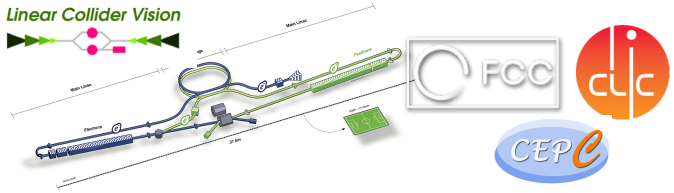

- Leading signal for light DM benchmarks Mono-Z + MET as in **DM55** and **DM70**.
- For heavier DM, associated bbH production channels takes over as in **DM156**.

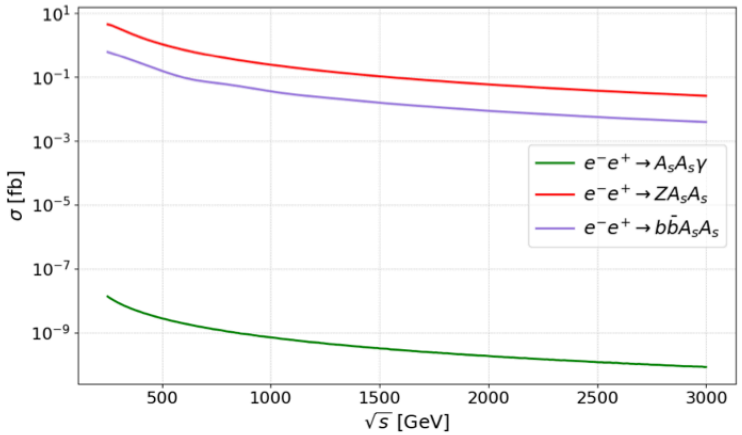

(a) $\mathbf{DM55_{w95}}$

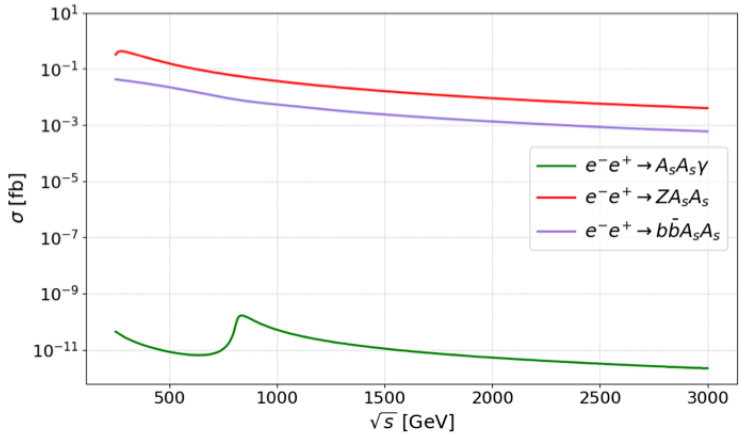

(b) $\mathbf{DM70}$

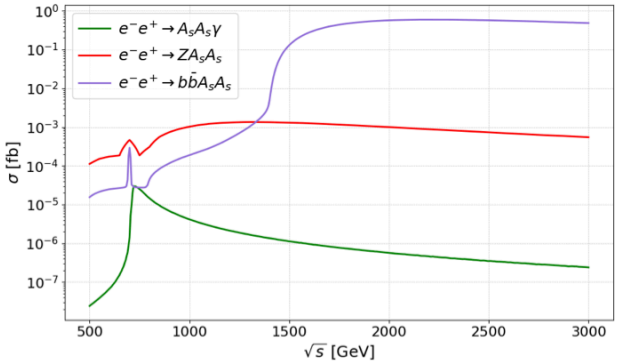

(c) $\mathbf{DM156_{w95}}$

Signals at e^+e^- colliders

Mono-Z + Missing Energy

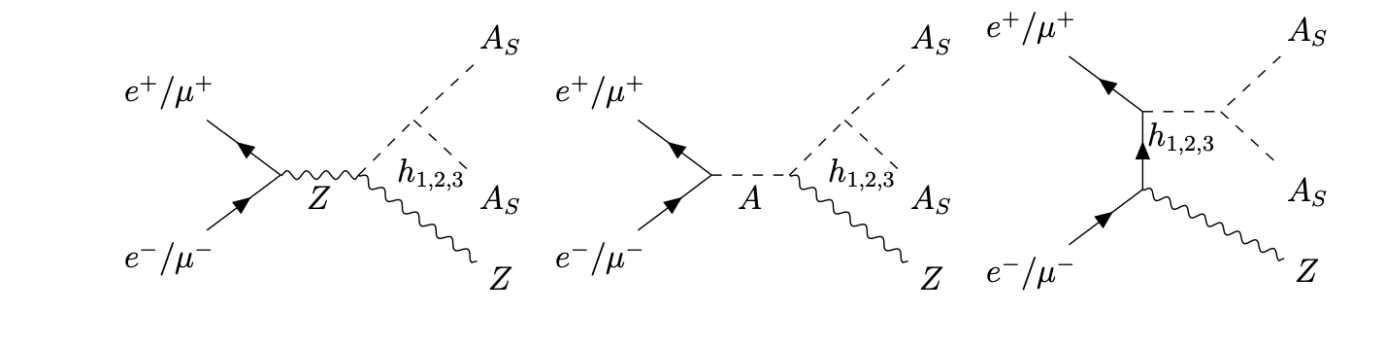

Benchmark	Production cross-section (fb)		
	At $\sqrt{s} = 250$ GeV	At $\sqrt{s} = 500$ GeV	At $\sqrt{s} = 1$ TeV
DM55$_{w95}$	4.42	1.1	0.24
DM70	0.33	0.15	0.035
$\nu\bar{\nu}Z$ background	503	491	950

Signal and dominant background Production cross sections at various center of mass energies at an unpolarised e+e- collider.

$\sqrt{s} = 250$ **GeV**

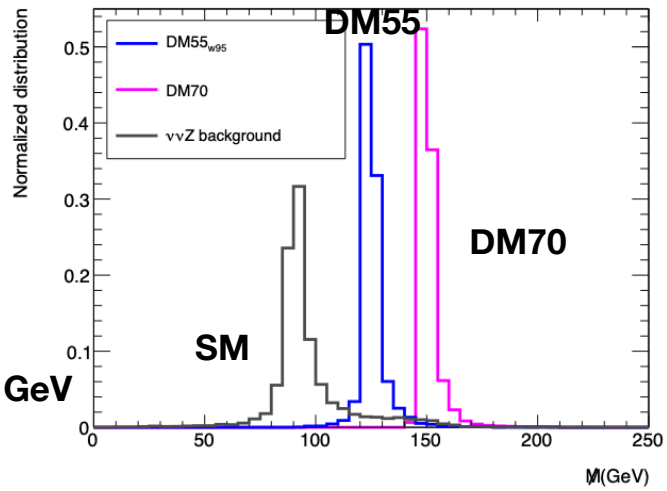

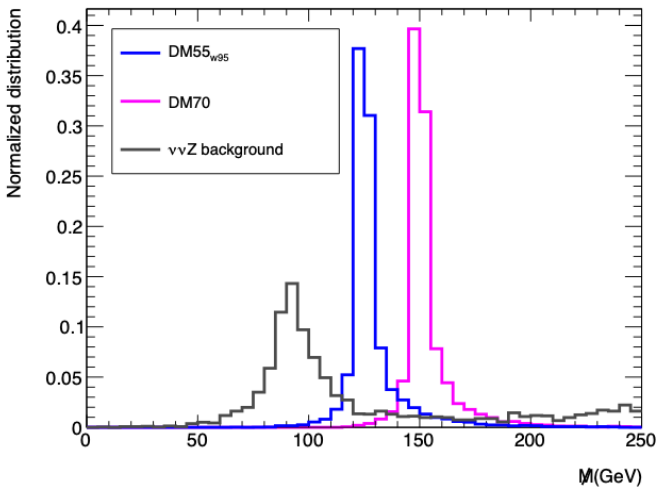

$\sqrt{s} = 500$ **GeV**

$\sqrt{s} = 1000$ **GeV**

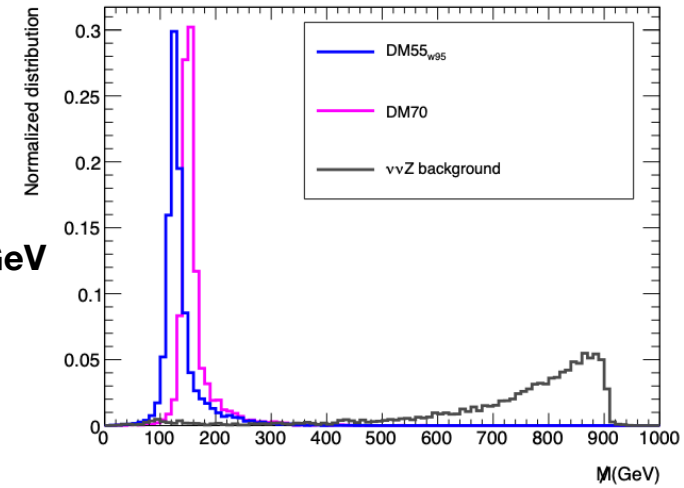

Missing Mass $\not{M}^2 = (p_{in} - p_{out})^2$

Powerful discriminator between signal and background.

Results

Light Dark Matter mostly sensitive via mono-Z + missing energy final state at a e+e- collider at 250 GeV.

Benchmark	$\sqrt{s}$	Cut	Significance
DM55$_{w95}$	250 GeV	$\not{M} > 100$ GeV	11σ (1 ab^{-1})
DM70	250 GeV	$\not{M} > 130$ GeV	3σ (3 ab^{-1})
DM55$_{w95}$	500 GeV	$\not{M} > 100$ GeV and $\not{M} < 150$ GeV	3.6σ (1 ab^{-1})
DM70	500 GeV	$\not{M} > 140$ GeV and $\not{M} < 190$ GeV	1.5σ (3 ab^{-1})
DM55$_{w95}$	1 TeV	$\not{M} > 120$ GeV and $\not{M} < 250$ GeV	2.4σ (3 ab^{-1})
DM70	1 TeV	$\not{M} > 120$ GeV and $\not{M} < 250$ GeV	0.36σ (3 ab^{-1})

Linear colliders are crucial to discover light DM in cases where LHC still hides it!

Dutta, et.al, 2504.14529

At $\mu^+\mu^-$colliders:

Relevant processes at muon colliders

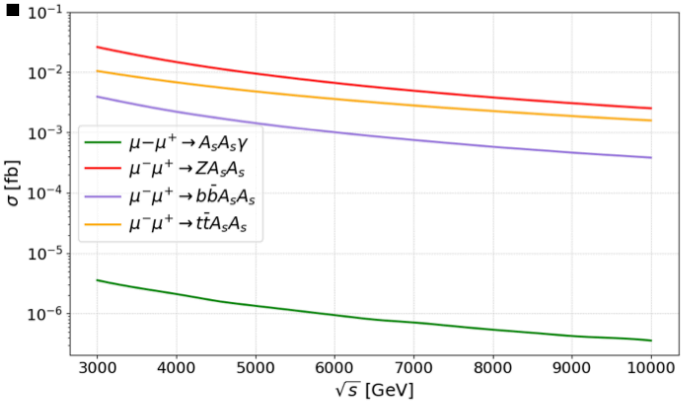

(a) **DM55$_{\mathbf{w95}}$**

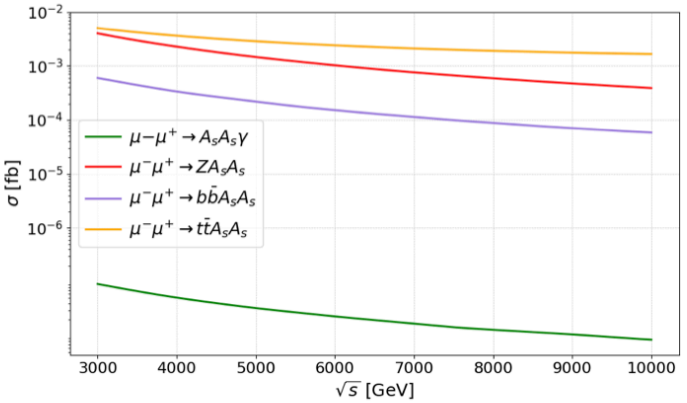

(b) **DM70**

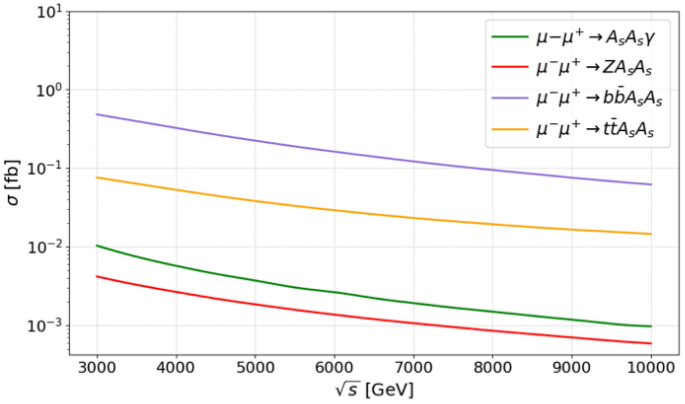

(c) **DM156$_{\mathbf{w95}}$**

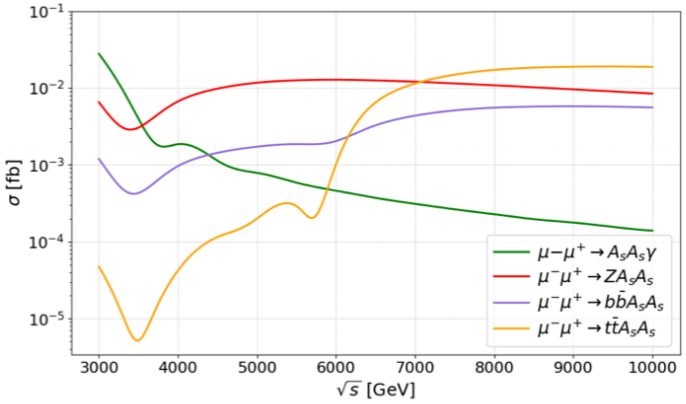

(d) **DM1000$_{\mathbf{w95}}$**

Intermediate DM

Heavy and Intermediate DM benefit from associated production modes such as bbH and ttH at higher energy lepton colliders/proposed muon colliders.

bb + Missing Energy (3 and 10TeV muon collider)

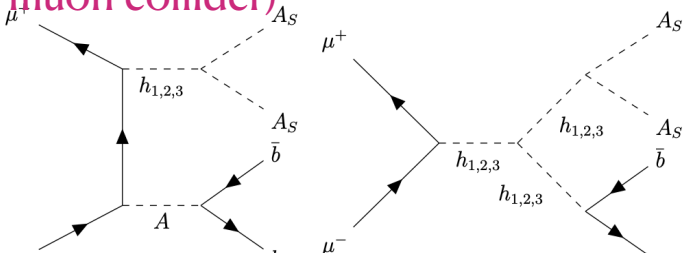

Benchmark	Cut	Significance
DM156$_{w95}$	100 GeV $< m_{bb} <$ 500 GeV	6.3σ $(3ab^{-1})$

Benchmark	Cut	Significance
DM156$_{w95}$	690 GeV $< \not{M} <$ 710 GeV	3σ $(3ab^{-1})$, 5.3σ $(10ab^{-1})$

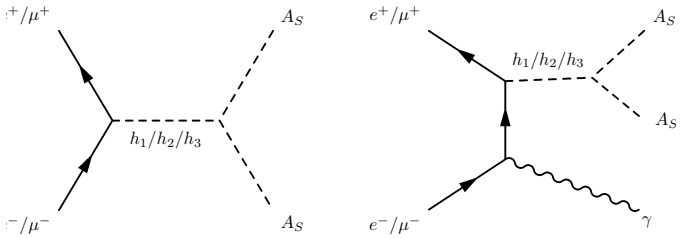

Mono $\not{\gamma}$ + Missing Energy (1 TeV muon collider)

Benchmark	Production cross-section (fb)at $\sqrt{s} = 1$ TeV
DM156$_{w95}$	0.23
$\nu\nu\gamma$ background	2.45

Cut	Significance
GeV $< \not{M} <$ 710 GeV	3σ $(3ab^{-1})$, 5.3σ $(10ab^{-1})$

Heavy DM

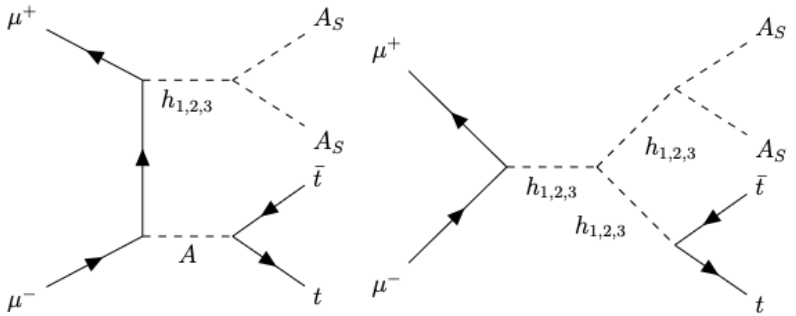

tt + Missing Energy

(10 TeV muon collider)

Benchmark	Production cross-section (fb) at $\sqrt{s} = 10$ TeV
DM1000$_{w95}$	0.027
$t\bar{t}$+MET background	1.66

Benchmark	Cut	Significance
DM1000$_{w95}$	$m_{bb} < 2$ TeV	2.9σ $(10ab^{-1})$

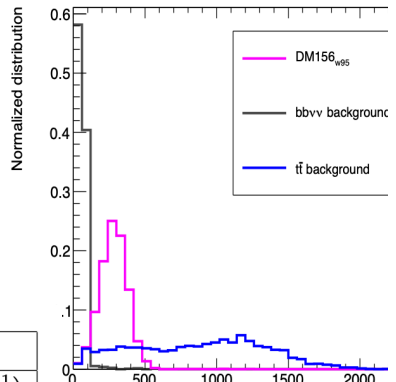

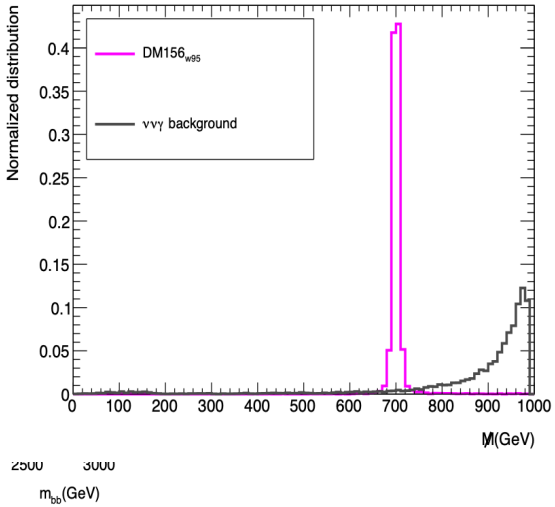

At $\mu^+\mu^-$colliders:

Relevant processes at muon colliders

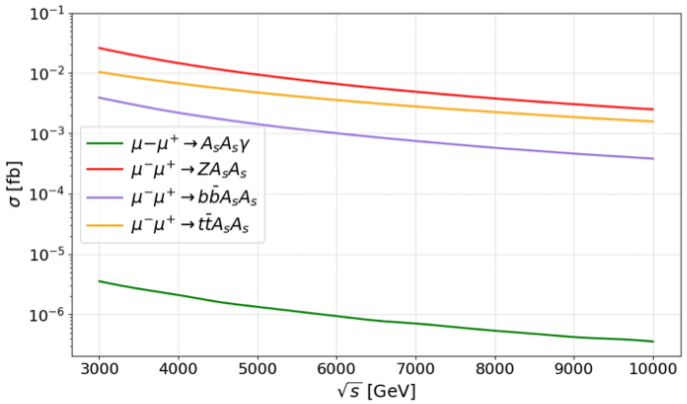

(a) **DM55$_{\mathbf{w95}}$**

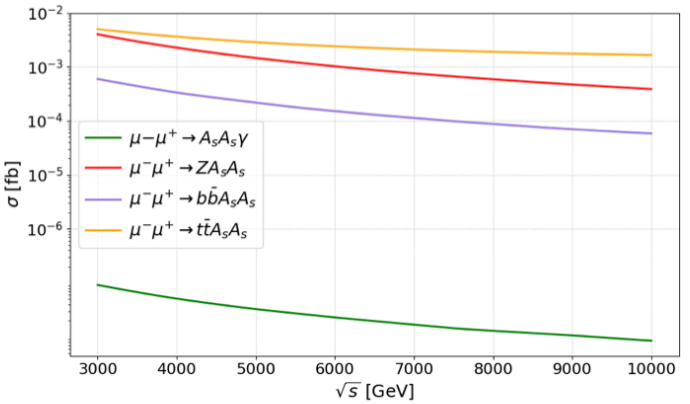

(b) **DM70**

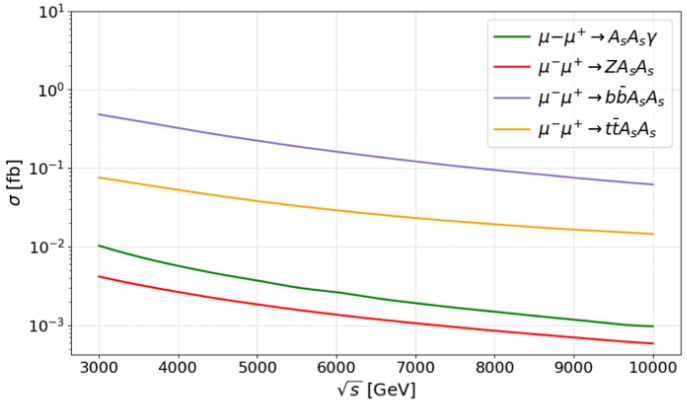

(c) **DM156$_{\mathbf{w95}}$**

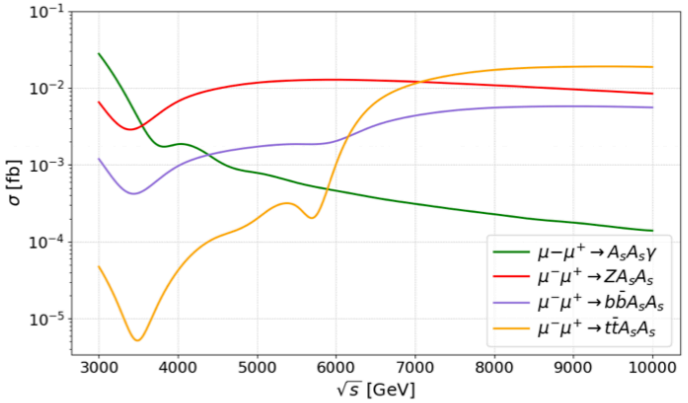

(d) **DM1000$_{\mathbf{w95}}$**

Intermediate DM

Heavy and Intermediate DM benefit from associated production modes such as bbH and ttH at higher energy lepton colliders/proposed muon colliders.

bb + Missing Energy (3 and 10TeV muon collider)

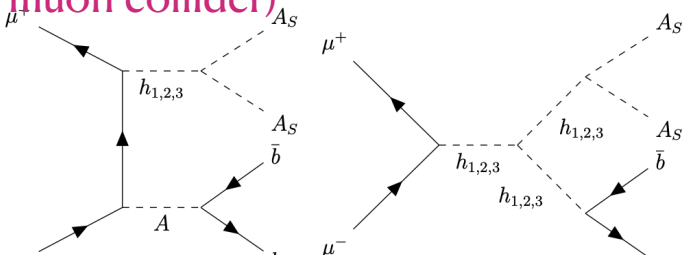

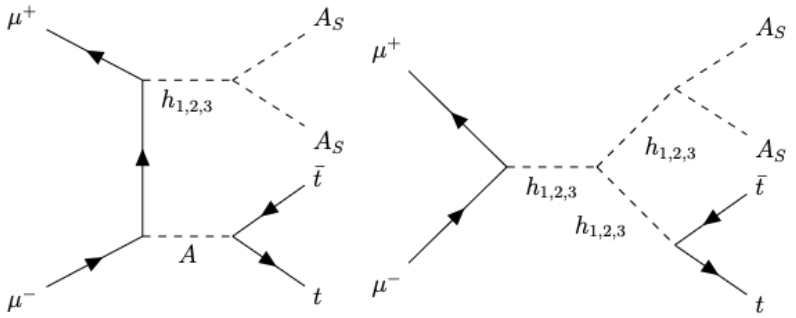

Heavy DM

tt + Missing Energy

(10 TeV muon collider)

Benchmark	Cut	Significance
DM156$_{w95}$	100 GeV $< m_{bb} <$ 500 GeV	6.3σ $(3ab^{-1})$

Benchmark	Cut	Significance
DM156$_{w95}$	690 GeV $< \not{M} <$ 710 GeV	3σ $(3ab^{-1})$, 5.3σ $(10ab^{-1})$

Benchmark	Production cross-section (fb) at $\sqrt{s} = 10$ TeV
DM1000$_{w95}$	0.027
$t\bar{t}$+MET background	1.66

Benchmark	Cut	Significance
DM1000$_{w95}$	$m_{bb} <$ 2 TeV	2.9σ $(10ab^{-1})$

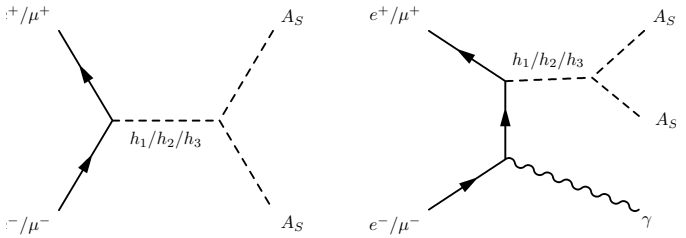

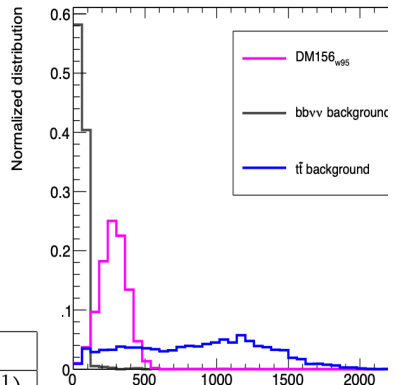

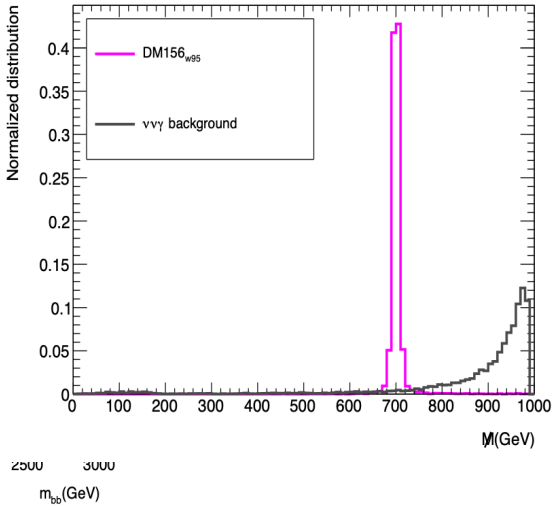

Mono $\not{\gamma}$ + Missing Energy (1 TeV muon collider)

Benchmark	Production cross-section (fb)at $\sqrt{s} = 1$ TeV
DM156$_{w95}$	0.23
$\nu\nu\gamma$ background	2.45

Cut	Significance
GeV $< \not{M} <$ 710 GeV	3σ $(3ab^{-1})$, 5.3σ $(10ab^{-1})$

Multicomponent DM in 2HDMS

	$U(1)$	$U(\not 1)$
Free parameters	$m_S^{2'}, \lambda_1'', \lambda_4', \lambda_5' = 0$	$m_S^{2'}, \lambda_1'', \lambda_4', \lambda_5' \neq 0$
Mass of DM	$m_{h_s} = m_{a_s}$	$m_{h_s} \neq m_{a_s}$
DM candidates	S	h_s, a_s

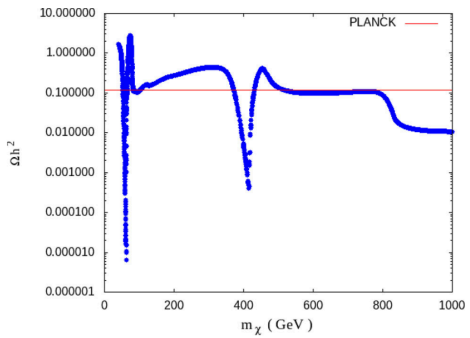

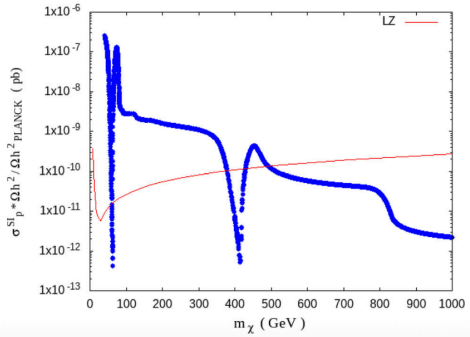

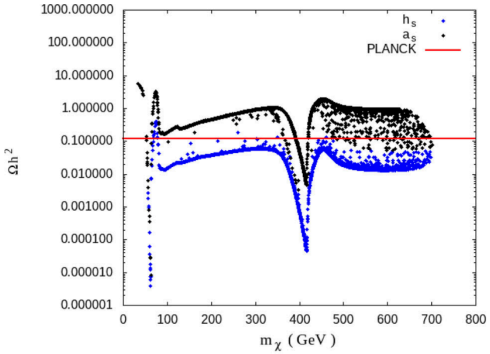

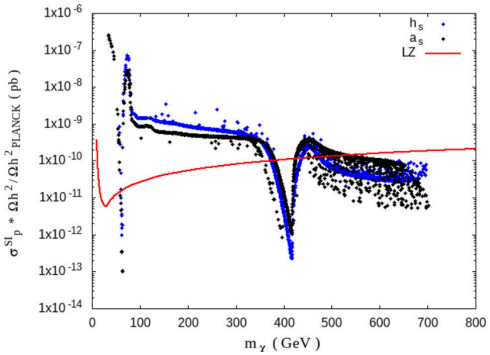

Dutta et.al,Eur.Phys.J.Plus 140 (2025) 1, 87

For heavy DM, dominant contributions from ttH and HA in 2b + Missing Energy final states.

$$e^- e^+ \to t\bar{t}H, \quad HA$$

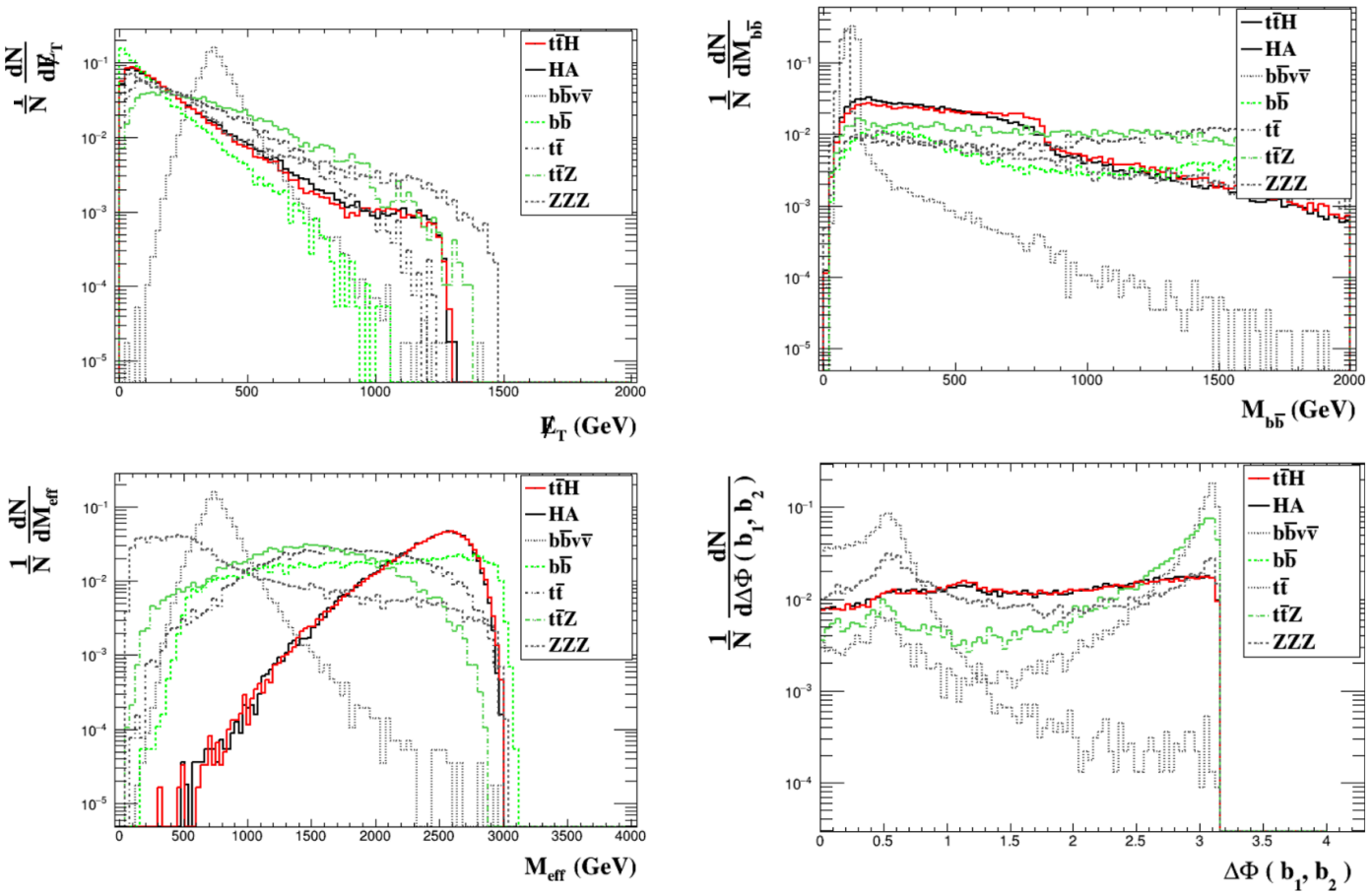

For heavy degenerate DM masses~400 GeV and Heavy Higgs mass ~ 833 GeV (with ~4% invisible branching) signal significance of $\sim 2.74\sigma$ at an e^+e^- collider at $\sqrt{s} = 3$ TeV at 5ab^{-1}

More detailed collider studies ongoing to explore full potential of multicomponent DM at higher energy linear colliders at 3 TeV!

Light Vector Boson Dark Matter in 2HDMS

$$m_{h_1}, m_{h_2}, m_{h_3}, m_{H^\pm}, m_A, m_{12}^2, \tan\beta, \sin\alpha_1, \sin\alpha_2, \sin\alpha_3, m_{DM}, g_x$$

$$\frac{dY_{Z'}}{dx} = \langle\sigma v\rangle_{Z'Z'\to XY}\frac{\beta s}{\mathcal{H}x}(Y_{Z'}^2 - Y_{Z'}^{eq2})$$

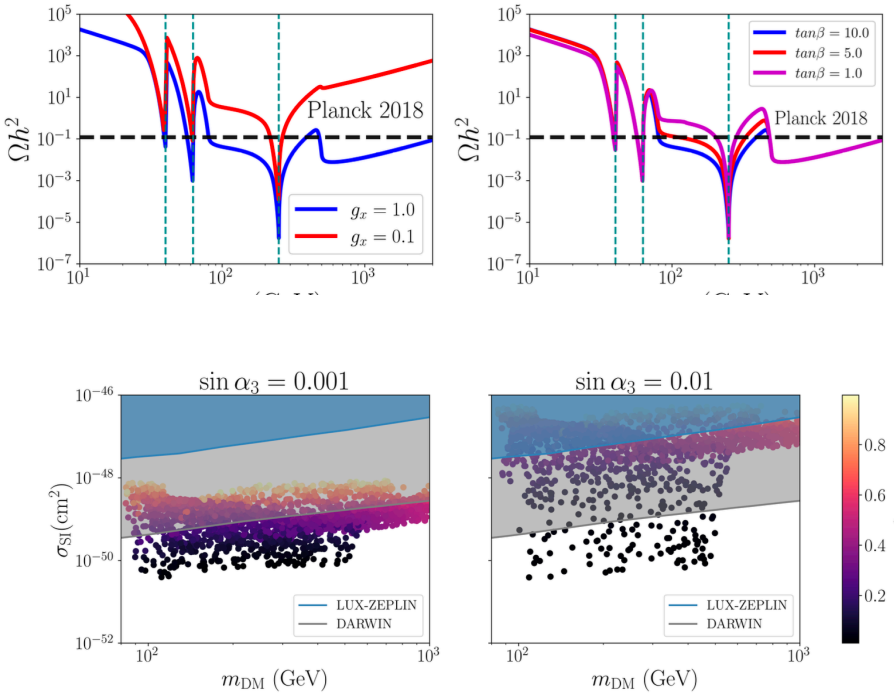

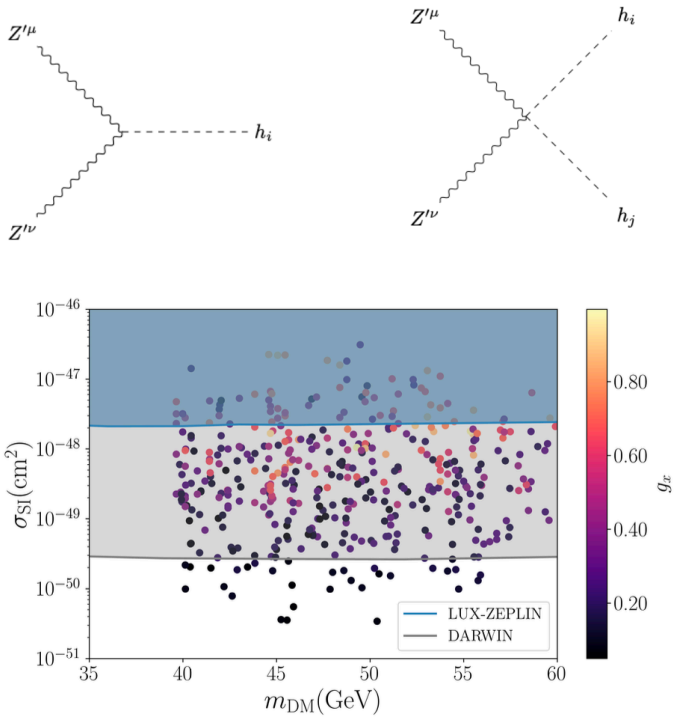

Light DM in the range 40-60 GeV (in the most constrained regions from LZ direct detection data) in Type I 2HDM + S extension with U(1)X symmetry.

Das, Dutta, Ghosh, Rai, Phys.Rev.D 112 (2025) 11, 115036

Current and Proposed Future experiments

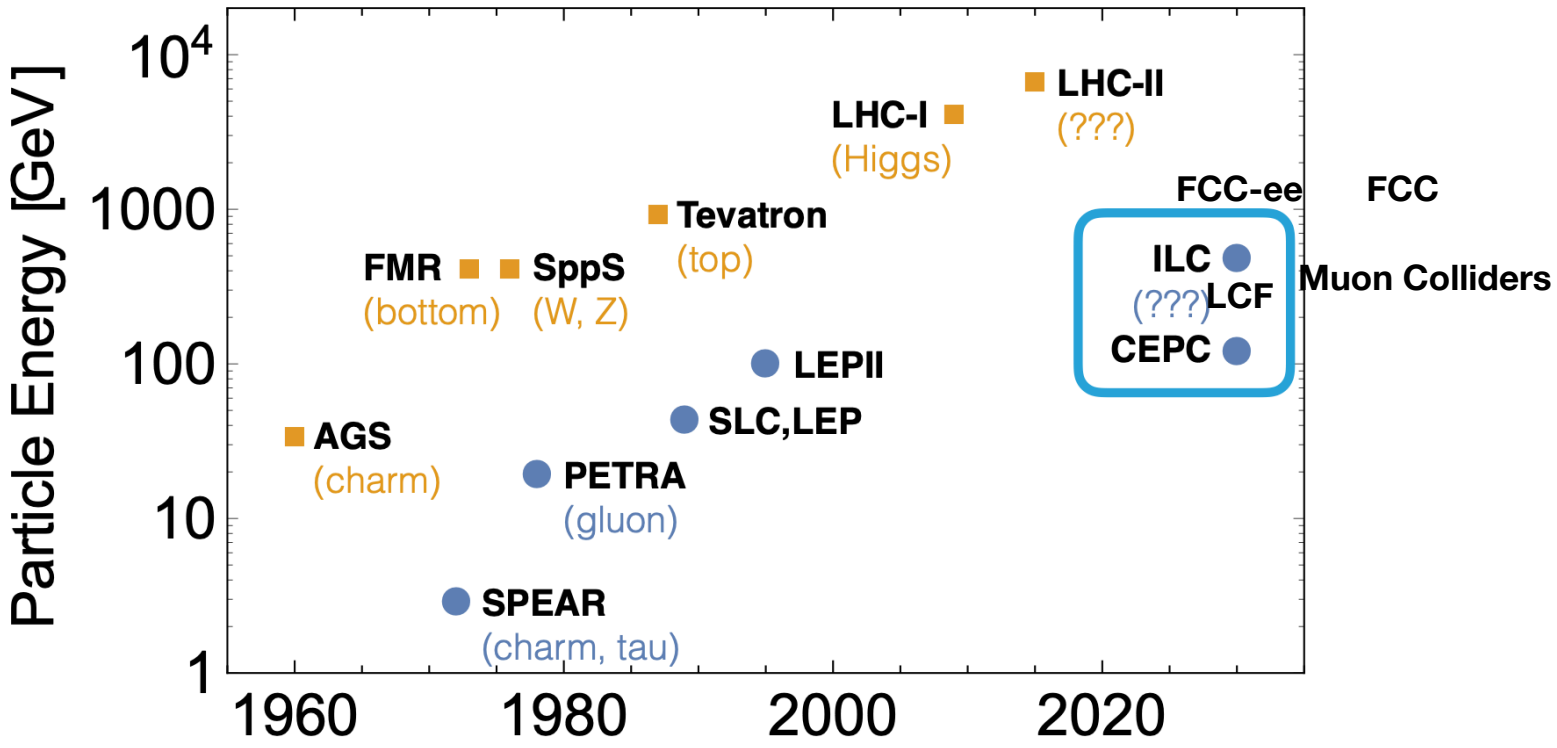

CERN.

Synergy between different colliders crucial to discover new physics scenarios.

Summary

- **Dark Matter remains one of the most challenging yet intriguing mysteries of Nature.**
- Extended Higgs portals models accommodating dark matter (such as the Type II 2HDM extended with a complex singlet scalar) very well motivated and **connects Particle Physics at low scale and the early Universe cosmology.**
- **Exciting signals which are hinted at HL-LHC, decisively detected at lepton colliders such as for light pseudoscalar DM at an e^+e^- collider of 250 GeV via the Higgsstrahlung process using missing mass reconstruction techniques.**
- **Associated production channels bbH, ttH, HA take over for heavy and intermediate DM cases at higher center of mass energies (~3 TeV) and beneficial to look for at higher energy lepton colliders akin to muon colliders to enhance reach of BSM higgs searches.**
- Potential for high energy lepton colliders to uncover multi-component DM at 3 TeV e+e- colliders for heavier DM masses. -> Ongoing work to explore full potential of multicomponent DM reach!

Thank You!

Couplings in 2HDM

The reduced Higgs to fermion couplings for all four Yukawa types are summarized in Tab. 1.

	type I	type II	lepton-specific	flipped
$c_{h_i tt}$	$\frac{R_{i2}}{\sin\beta}$	$\frac{R_{i2}}{\sin\beta}$	$\frac{R_{i2}}{\sin\beta}$	$\frac{R_{i2}}{\sin\beta}$
$c_{h_i bb}$	$\frac{R_{i2}}{\sin\beta}$	$\frac{R_{i1}}{\cos\beta}$	$\frac{R_{i2}}{\sin\beta}$	$\frac{R_{i1}}{\cos\beta}$
$c_{h_i \tau\tau}$	$\frac{R_{i2}}{\sin\beta}$	$\frac{R_{i1}}{\cos\beta}$	$\frac{R_{i1}}{\cos\beta}$	$\frac{R_{i2}}{\sin\beta}$

Table 1: Higgs to fermion reduced couplings for different type of Yukawa couplings

Gauge couplings in 2HDM $c_{h_i VV} = c_{h_i ZZ} = c_{h_i WW} = \cos\beta R_{i1} + \sin\beta R_{i2}$

Branco, et.al,
https://doi.org/10.1016/j.physrep.2012.02.002

Benchmarks

m_{h_1}	m_{h_2}	m_{h_3}	m_A	$m_{H^\pm}$	χ^2
95.4 GeV	125.09 GeV	650 GeV	800 GeV	800 GeV	1.26
m_{A_S}	$\lambda_1' - 2\lambda_4'$	$\lambda_2' - 2\lambda_5'$	$\lambda_1'' - \lambda_3''$	$\tan\beta$	
55.596 GeV	0.0020912	0.00074611	−0.025735	2	
v_S	$\tilde{\mu}$	α_1	α_2	α_3	
300 GeV	650 GeV	−1.932	1.272	1.484	

DM55_w95

m_{h_1}	m_{h_2}	m_{h_3}	m_A	$m_{H^\pm}$
800 GeV	125.09 GeV	150 GeV	800 GeV	800 GeV
m_{A_S}	$\lambda_1' - 2\lambda_4'$	$\lambda_2' - 2\lambda_5'$	$\lambda_1'' - \lambda_3''$	$\tan\beta$
70 GeV	−0.10783	0.063127	−0.47818	1.3728
v_S	$\tilde{\mu}$	α_1	α_2	α_3
219.05 GeV	751.54 GeV	−0.60016	0.042445	−0.054807

DM70

m_{h_1}	m_{h_2}	m_{h_3}	m_A	$m_{H^\pm}$	χ^2
95.4 GeV	125.09 GeV	700 GeV	700 GeV	700 GeV	0.422
m_{A_S}	$\lambda_1' - 2\lambda_4'$	$\lambda_2' - 2\lambda_5'$	$\lambda_1'' - \lambda_3''$	$\tan\beta$	
156 GeV	12.753	−0.31351	−2.6747	6.6	
v_S	$\tilde{\mu}$	α_1	α_2	α_3	
239.86 GeV	700 GeV	1.4661	1.1920	−1.5989	

DM156_w95

m_{h_1}	m_{h_2}	m_{h_3}	m_A	$m_{H^\pm}$	χ^2
95.4 GeV	125.09 GeV	2950 GeV	2950 GeV	2950 GeV	2.13
m_{A_S}	$\lambda_1' - 2\lambda_4'$	$\lambda_2' - 2\lambda_5'$	$\lambda_1'' - \lambda_3''$	$\tan\beta$	
1000 GeV	21.231	0	−1.4153	5	
v_S	$\tilde{\mu}$	α_1	α_2	α_3	
10005 GeV	2949.29 GeV	−1.769	1.250	1.569	

DM1000_w95

Influence of portal couplings

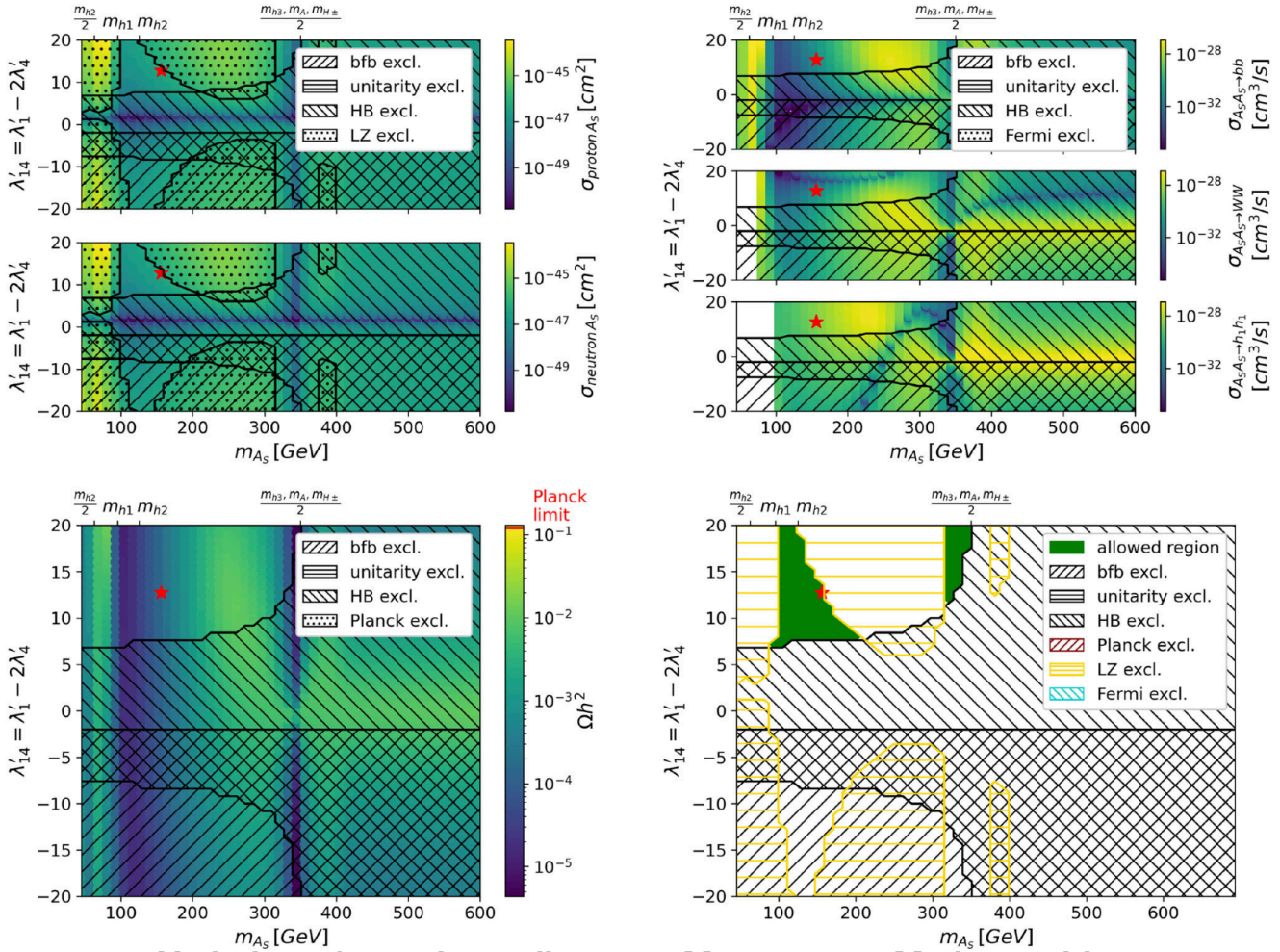

Variation of portal coupling vs. DM mass on DM observables.

Dutta et.al, *Eur.Phys.J.C 86 (2026) 4, 384*

LHC Cross-sections

Process	Production cross-section (fb) at $\sqrt{s} = 14$ TeV		
	DM55$_{\mathbf{w95}}$	**DM156$_{\mathbf{w95}}$**	**DM70**
GGF($h_2 \to A_S A_S$)	533.9	-	19.29×10^{3}
GGF($h_3 \to A_S A_S$)	-	0.015	-
VBF($h_2 \to A_S A_S$)	54.33	-	2.72×10^{3}
VBF($h_3 \to A_S A_S$)	-	0.134	0.0022
BBH ($(b\bar{b}h_2 \to A_S A_S)$)	21.6	-	0.137
BBH ($(b\bar{b}h_3 \to A_S A_S)$)	-	47.24	-

Table 4: The production cross-sections at leading order (LO) of the relevant processes at $\sqrt{s} = 14$ TeV at LHC. All cross-sections below 10^{-6} fb are denoted by '-'. For $b\bar{b}h_i$, with $i = 2, 3$, we use the Santander matched cross-section as defined in the text.

Process	Production cross-section (fb) at $\sqrt{s} = 14$ TeV		
	DM400	**DM1000**	**DM1000$_{\mathbf{w95}}$**
GGF($h_3 \to A_S A_S$)	0.013	6.35×10^{-7}	4.5×10^{-6}
VBF($h_3 \to A_S A_S$)	0.0008	-	-
BBH($h_3 \to A_S A_S$)	0.007	-	-

Basis Change

$$
\begin{aligned}
m_{12}^2 &= \tilde{\mu}^2 \cdot \sin\beta\cos\beta, \\
\lambda_1 &= \frac{1}{v^2\cos^2\beta}(\Sigma_{i=1}^3 m_i^2 R_{i1}^2 - \tilde{\mu}^2\sin^2\beta), \\
\lambda_2 &= \frac{1}{v^2\sin^2\beta}(\Sigma_{i=1}^3 m_i^2 R_{i2}^2 - \tilde{\mu}^2\cos^2\beta), \\
\lambda_3 &= \frac{1}{v^2}\left(\frac{1}{\sin\beta\cos\beta}\Sigma_{i=1}^3 m_i^2 R_{i1}R_{i2} - \tilde{\mu}^2 + 2m_{H^\pm}^2\right), \\
\lambda_4 &= \frac{1}{v^2}(m_A^2 + \tilde{\mu}^2 - 2m_{H^\pm}^2), \\
\lambda_5 &= \frac{1}{v^2}(-m_A^2 + \tilde{\mu}^2), \\
\lambda_1' &= \frac{1}{2}\left(\frac{1}{vv_S\cos\beta}\Sigma_{i=1}^3 m_i^2 R_{i1}R_{i3} + \lambda_{14}'\right), \\
\lambda_2' &= \frac{1}{2}\left(\frac{1}{vv_S\sin\beta}\Sigma_{i=1}^3 m_i^2 R_{i2}R_{i3} + \lambda_{25}'\right), \\
\lambda_4' &= \frac{1}{4}\left(\frac{1}{vv_S\cos\beta}\Sigma_{i=1}^3 m_i^2 R_{i1}R_{i3} - \lambda_{14}'\right),
\end{aligned}
$$

$$
\begin{aligned}
\lambda_5' &= \frac{1}{4}\left(\frac{1}{vv_S\sin\beta}\Sigma_{i=1}^3 m_i^2 R_{i2}R_{i3} - \lambda_{25}'\right), \\
\lambda_1'' &= \lambda_{13}'' + \lambda_3'', \\
\lambda_3'' &= \frac{3}{4v_S^2}(\Sigma_{i=1}^3 m_i^2 R_{i3}^2 - \lambda_{13}''v_S^2 - 4\lambda_2''v_S^2), \\
m_S'^2 &= -\left(\frac{1}{2}m_{A_S}^2 + \frac{1}{4}\Sigma_{i=1}^3 m_i^2\left(R_{i3}^2 + R_{i1}R_{i3}\frac{v\cos\beta}{v_S}\right.\right. \\
&\quad \left. + R_{i2}R_{i3}\frac{v\sin\beta}{v_S}\right) - \frac{v^2}{4}(\lambda_{14}'\cos^2\beta \\
&\quad \left.\left. + \lambda_{25}'\sin^2\beta) + \frac{v_S^2}{8}\lambda_{13}''\right),
\end{aligned}
$$

Rotation Matrix

$$
R = \begin{pmatrix}
c_{\alpha_1}c_{\alpha_2} & s_{\alpha_1}c_{\alpha_2} & s_{\alpha_2} \\
-s_{\alpha_1}c_{\alpha_3} - c_{\alpha_1}s_{\alpha_2}s_{\alpha_3} & c_{\alpha_1}c_{\alpha_3} - s_{\alpha_1}s_{\alpha_2}s_{\alpha_3} & c_{\alpha_2}s_{\alpha_3} \\
s_{\alpha_1}s_{\alpha_3} - c_{\alpha_1}s_{\alpha_2}c_{\alpha_3} & -c_{\alpha_1}s_{\alpha_3} - s_{\alpha_1}s_{\alpha_2}c_{\alpha_3} & c_{\alpha_2}c_{\alpha_3}
\end{pmatrix},
$$

Dutta, et.al, Eur.Phys.J.Plus 140 (2025) 1, 87

Benchmark	Production cross-section (fb)	
	at $\sqrt{s} = 3$ TeV	at $\sqrt{s} = 10$ TeV
DM156$_{\mathbf{w95}}$	0.48	0.063
$b\bar{b}\nu\nu$ background	758	1.3
$t\bar{t}$ background	20	1.7

bb+Missing Energy cross-sections at Muon Colliders.

Benchmark	Production cross-section (fb)		
	at $\sqrt{s} = 250$ GeV	at $\sqrt{s} = 500$ GeV	at $\sqrt{s} = 1$ TeV
DM55$_{\mathbf{w95}}$	4.42	1.1	0.24
DM70	0.33	0.15	0.035
$\nu\bar{\nu}Z$ background	503	491	950

Mono Z + Missing energy cross-sections at Muon Colliders.

	Ωh^2	σ_{pA_S}/pb	σ_{nA_S}/pb	$\sigma_{A_SA_S\to XX}/\frac{\text{cm}^3}{\text{s}}$	$BR(h_3 \to A_SA_S)$	$BR(h_2 \to A_SA_S)$
DM55$_{\mathbf{w95}}$	0.11	4.21×10^{-12}	4.08×10^{-12}	1.98×10^{-28}	3.81×10^{-9}	0.0199
DM156$_{\mathbf{w95}}$	1.61×10^{-4}	3.903×10^{-11}	4.160×10^{-11}	3.875×10^{-29}	0.69	-
DM1000$_{\mathbf{w95}}$	0.111	3.323×10^{-11}	3.369×10^{-11}	2.045×10^{-26}	0.0359	-
DM70	0.113	8.938×10^{-16}	2.651×10^{-13}	2.13×10^{-28}	0.99934	-
DM400	0.106	4.960×10^{-11}	5.101×10^{-11}	3.67×10^{-26}	0.82203	-
DM1000	0.117	$8.263 \cdot 10^{-11}$	$8.464 \cdot 10^{-11}$	$2.018 \cdot 10^{-26}$	0.005	-

Allowed Benchmarks

Benchmark

Parameters	**BP3**
λ_1	0.21
λ_2	0.26
λ_3	0.25
λ_4	–0.1
λ_5	0.1
$\lambda_1^{''m}$	0.01
$\lambda_2^{''m}$	0.0001
$\lambda_3^{''m}$	0.001
$\lambda_1^{'m}$	2.0
$\lambda_2^{'m}$	0.1
$\lambda_4^{'m}$	–0.1
$\lambda_5^{'m}$	-0.1
$m_{12}^2(\text{GeV}^2)$	1.0×10^5
$m_{DM_1}^2(\text{GeV}^2)$	300000
$m_{DM_2}^2(\text{GeV}^2)$	380000
$\tan\beta$	6.8
$\cos(\alpha-\beta)$	–0.00015
m_h (GeV)	125.6
m_H(GeV)	833.5
m_A(GeV)	829.8
$m_{H^\pm}$ (GeV)	833.5
m_{a_s} (GeV)	398.12
m_{h_s} (GeV)	428.88
BR($H\to a_s a_s$)	3.9×10^{-2}
Ωh^2	1.03×10^{-3}
$\sigma_p^{SI} * \frac{\Omega h^2}{\Omega h^2_{PLANCK}}$ ($\times10^{11}$ pb)	2.66
$\sigma_n^{SI} * \frac{\Omega h^2}{\Omega h^2_{PLANCK}}$ ($\times10^{11}$ pb)	2.79

Backgrounds and cuts for multicomponent DM

We study the final state of $2b+\not{E}_T$ with the missing energy arising from $H \to \chi\bar{\chi}$ at an unpolarized e^+e^- collider for an integrated luminosity of $\mathcal{L} = 5$ ab^{-1}. Dominant SM background contributions arise from

- $b\bar{b}$ (for misidentification of decay products of b-quark along with missing energy from b decays)
- $b\bar{b}\nu\bar{\nu}$ (including both on-shell and off-shell contribution from Z boson decay as well as $\nu\bar{\nu}h$ contribution)
- $Z(\to b\bar{b})Z(\to \nu\bar{\nu})$
- hZ $(h \to b\bar{b},\ Z \to \nu\bar{\nu})$
- $t\bar{t}Z$, $(Z \to \nu\bar{\nu},\ t \to bW^+)$ for misidentified leptons/jets from W bosons.
- Leptonic $t\bar{t}$ for misidentified leptons or semi-leptonic $t\bar{t}$ decays with missing energy arising from the b decaying leptonically.
- WWZ
- ZZZ

Cuts for analysis: 2b + MET

- **C1**: The final state consists of two b-jets and no leptons or photons.
- **C2**: The leading b-jet has transverse momentum $p_T > 100$ GeV and sub-leading b-jet has $p_T > 80$ GeV. The hard p_T cuts on the b-jets help to reduce backgrounds from SM backgrounds from Z and h bosons.
- **C3**: The invariant mass of the two b-jets within the mass window 80 GeV $< M_{b_1 b_2} <$130 GeV is rejected to remove contributions from Z and h bosons.

- **C4**: Since the dark matter is heavy, we demand a large cut on the effective mass $M_{eff} > 1.2$ TeV where $M_{eff} = \sum_i (p_{T_i}) + \not{E}_T$.
- **C5**: Further, we demand $\not{E}_T > 650$ GeV on the final state which reduces the dominant SM backgrounds.
- **C6**: The $\Delta\Phi$ between two b-jets is significantly different for the signal and background from $b\bar{b}$ where the b-jets are mostly back-to-back. We demand $\Delta\Phi(b_1, b_2) < 1.60$. This also reduces the backgrounds from $b\bar{b}$ as well as from $t\bar{t}$ and $t\bar{t}Z$ sharply.

Light Vector Boson Dark Matter in 2HDMS

$$Z_2^{(A)}:\ Z'_\mu \to -Z'_\mu, S \to S^*, \qquad Z_2^{(B)}: Z'_\mu \to -Z'_\mu, S \to -S^*$$

$$\begin{aligned}
&V(\Phi_1,\Phi_2,S)\\
&= m_{11}^2(\Phi_1^\dagger\Phi_1) + m_{22}^2(\Phi_2^\dagger\Phi_2) + m_{33}^2(S^*S)\\
&\quad - [m_{12}^2(\Phi_1^\dagger\Phi_2) + \text{H.c.}] + \lambda_1(\Phi_1^\dagger\Phi_1)^2\\
&\quad + \lambda_2(\Phi_2^\dagger\Phi_2)^2 + \lambda_S(S^*S)^2 + \lambda_3(\Phi_1^\dagger\Phi_1)(\Phi_2^\dagger\Phi_2)\\
&\quad + \lambda_4(\Phi_1^\dagger\Phi_2)(\Phi_2^\dagger\Phi_1) + \lambda_{S1}(\Phi_1^\dagger\Phi_1)(S^*S)\\
&\quad + \lambda_{S2}(\Phi_2^\dagger\Phi_2)(S^*S) + \Big\{\frac{1}{2}\lambda_5(\Phi_1^\dagger\Phi_2)^2\\
&\quad + [\lambda_6(\Phi_1^\dagger\Phi_1) + \lambda_7(\Phi_2^\dagger\Phi_2) + \lambda_8(S^*S)] \times (\Phi_1^\dagger\Phi_2) + \text{H.c.}\Big\},
\end{aligned}$$

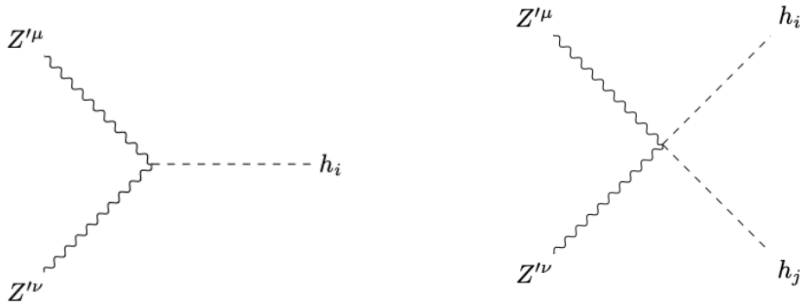

$$\lambda_{h_i Z' Z'} = 2 g_x^2 v_S \mathcal{R}_{i3}$$
$$\lambda_{Z' Z' h_i h_j} = 2 g_x^2 \mathcal{R}_{i3} \mathcal{R}_{j3}$$

Free parameters:

$$m_{h_1}, m_{h_2}, m_{h_3}, m_{H^\pm}, m_A, m_{12}^2, \tan\beta, \sin\alpha_1, \sin\alpha_2, \sin\alpha_3, m_{DM}, g_x$$

$$m_{\rm DM} = g_x v_S$$

Das, Dutta, Ghosh, Rai, Phys.Rev.D 112 (2025) 11, 115036

Light Vector Boson Dark Matter in 2HDMS

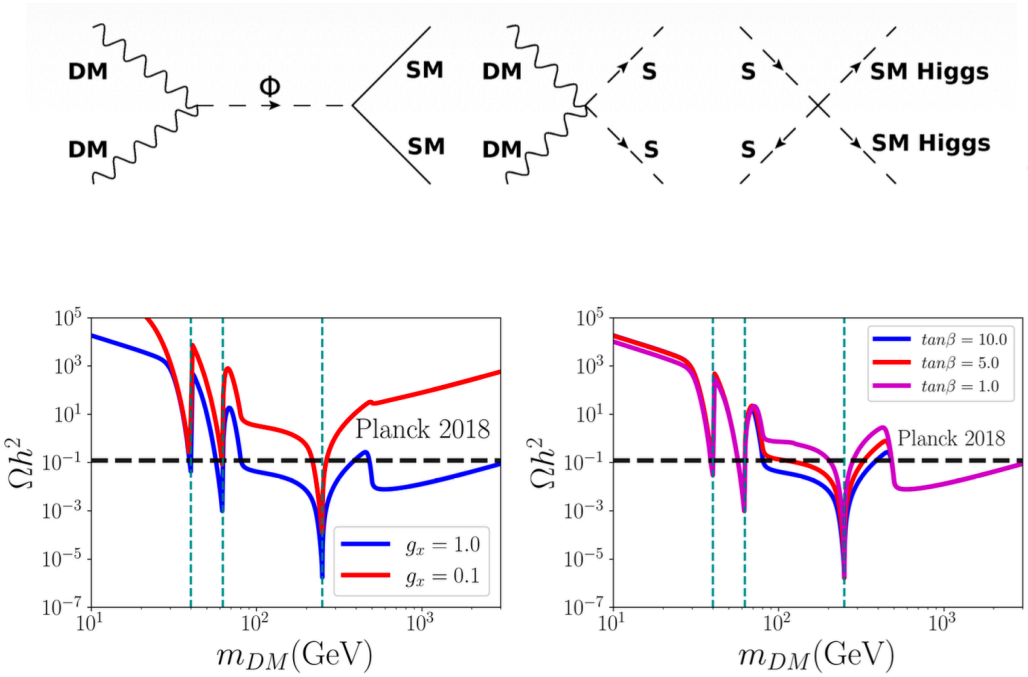

Figure 4. Relic abundance vs m_{DM} (GeV). The Higgs masses are fixed at $m_{h_1} = 80\,\text{GeV}, m_{h_2} = 125\,\text{GeV}, m_{h_3} = 500\,\text{GeV}$. In the left panel, two values of g_x are considered when $tan\beta = 10$. In the right panel, three values of $\tan\beta$ are considered when $g_x = 1.0$. The other parameters are fixed at $\sin\alpha_1 = 0.01$, $\sin\alpha_2 = 0.01$ and $\sin\alpha_3 = 0.01$.

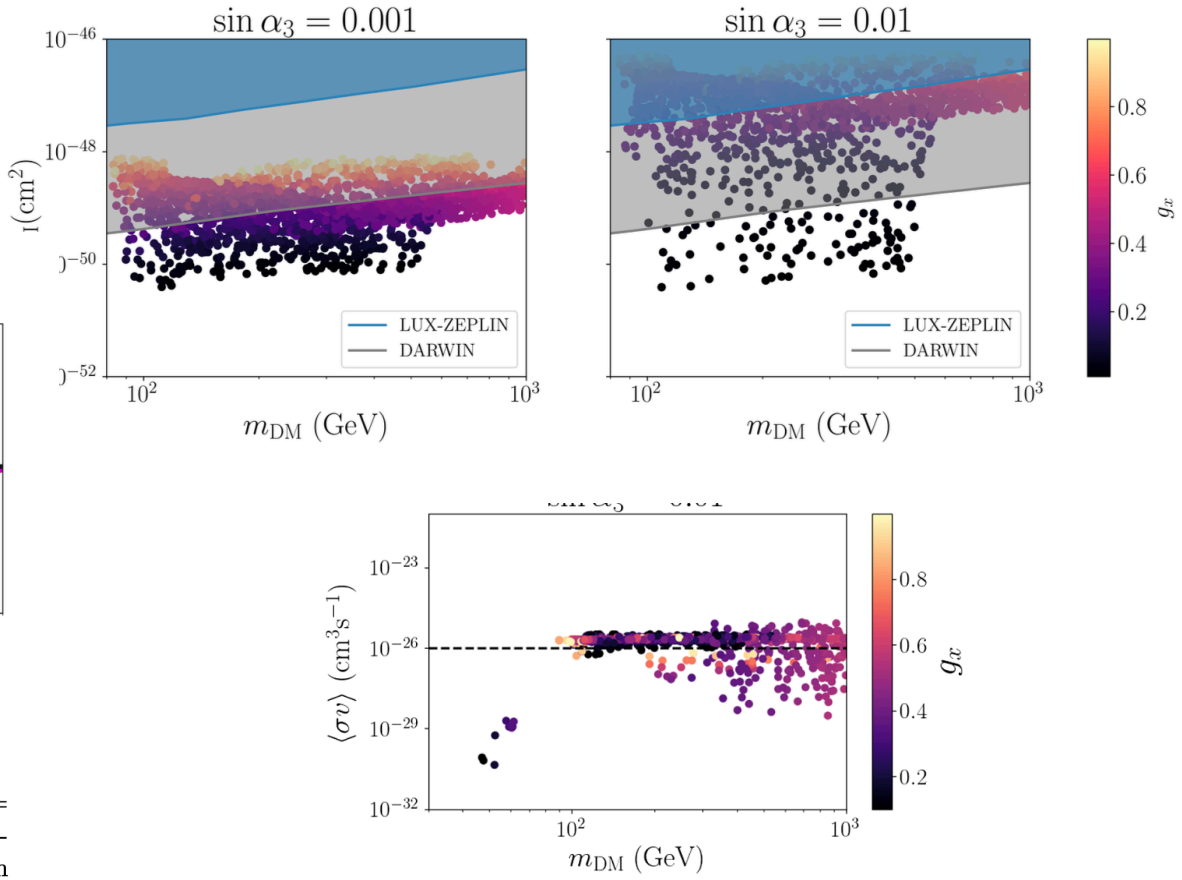

FIG. 8. Relic density satisfied parameter space in annihilation cross section vs $m_{\rm DM}$ plane.

Das, Dutta, Ghosh, Rai, Phys.Rev.D 112 (2025) 11, 115036

Light DM in the range 40-60 GeV (in the most constrained regions from LZ direct detection data) in Type I 2HDM + S extension with U(1)X symmetry.

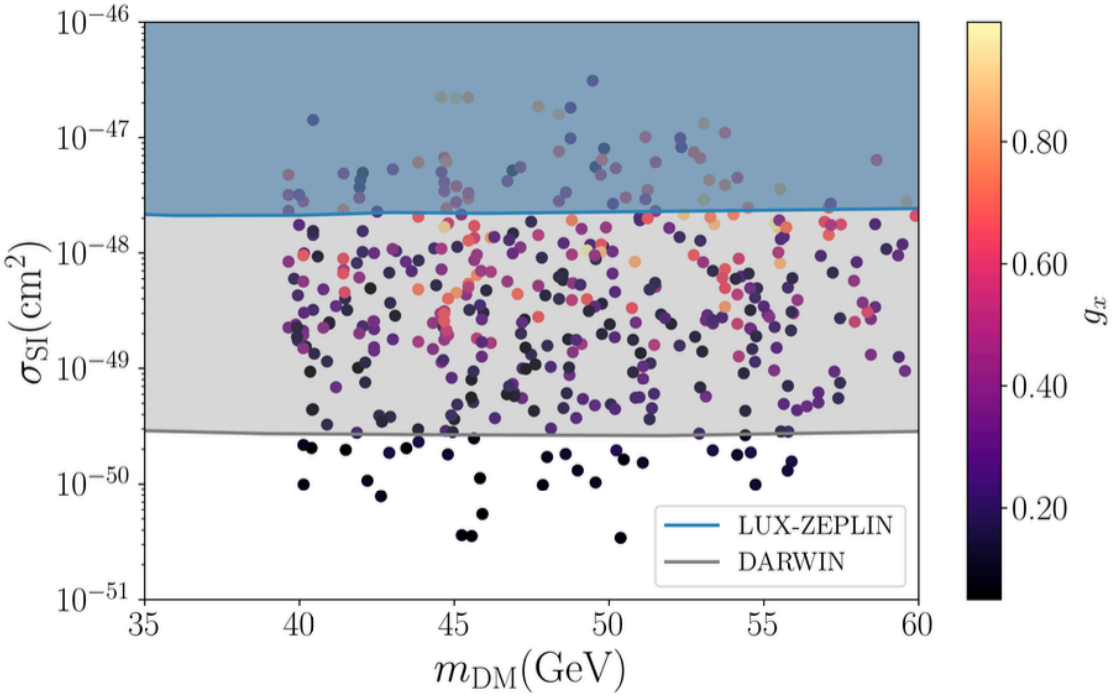

Feebly Interacting DM

$$\frac{dY_{\rm DM}}{dx} = \frac{\langle \Gamma_{S\to \rm DM\ DM}\rangle}{\mathcal{H}x} Y_S^{eq}(x)$$

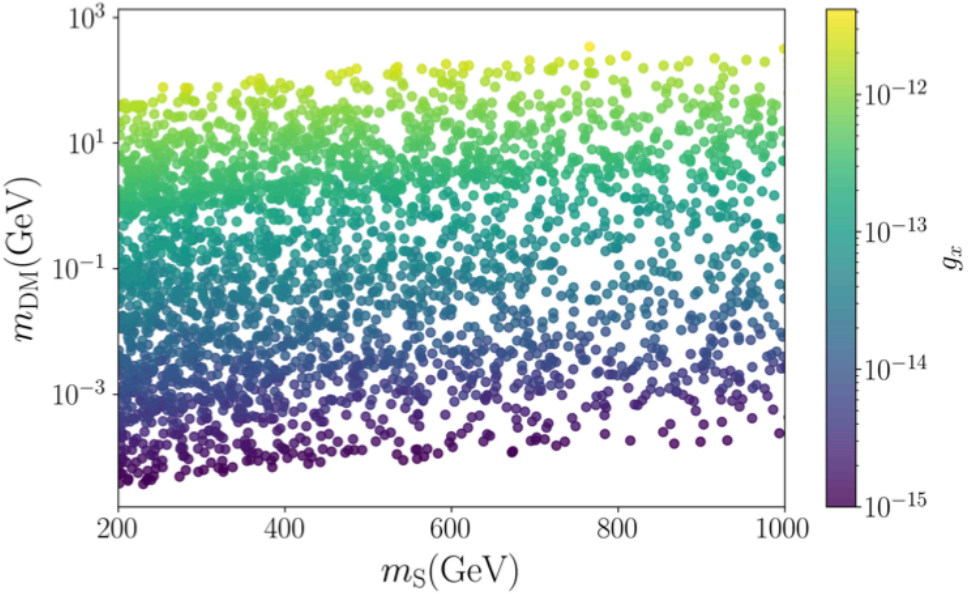

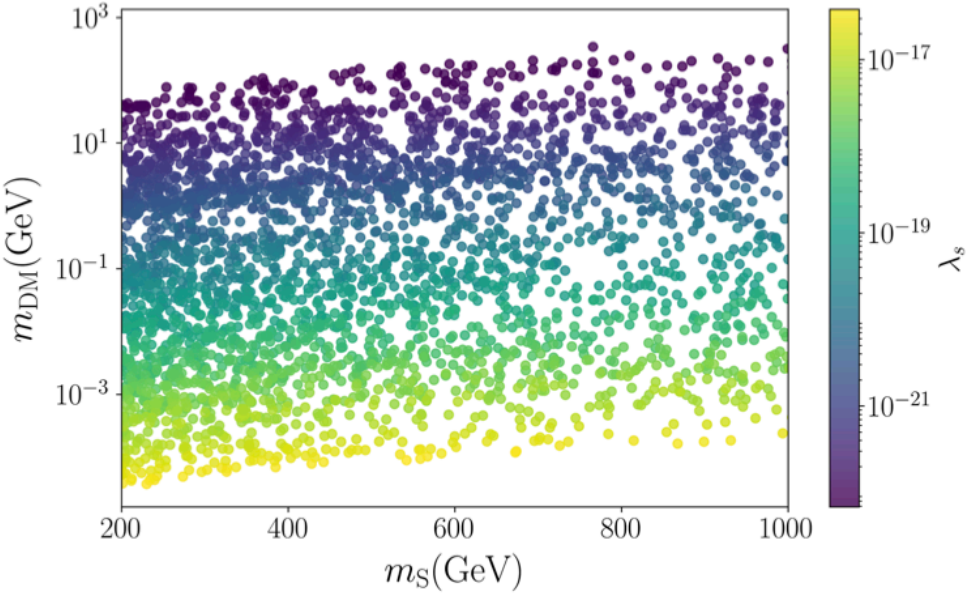

$$m_{\rm DM} = g_x v_S, \qquad m_S \sim \sqrt{\lambda_S} v_S$$

$$m_{\rm DM} \sim \frac{m_S g_x}{\sqrt{\lambda_S}}$$

Das, Dutta, Ghosh, Rai, Phys.Rev.D 112 (2025) 11, 115036

Representative Benchmarks

No.	g_x	m_{DM} (GeV)	m_{h_1} (GeV)	m_{h_3} (GeV)	$\sigma_{SI}(\mathrm{cm}^2)$
BP1	0.16	54.78	109.97	300.0	4.92×10^{-49}
BP2	0.20	44.35	89.74	300.0	1.08×10^{-48}
BP3	0.28	90.50	87.28	221.71	2.27×10^{-48}
BP4	0.35	177.64	101.30	530.84	6.71×10^{-48}
BP5	0.48	527.0	101.90	478.71	1.20×10^{-47}

No.	Annihilation channels	No.	Annihilation channels
BP1	$Z'Z' \to b\bar{b}(80\%)$ $Z'Z' \to c\bar{c}(12\%)$ $Z'Z' \to \tau\bar{\tau}(8\%)$	BP2	$Z'Z' \to b\bar{b}(80\%)$ $Z'Z' \to c\bar{c}(12\%)$ $Z'Z' \to \tau\bar{\tau}(8\%)$
BP3	$Z'Z' \to H^+H^-(42\%)$ $Z'Z' \to h_1h_1(35\%)$ $Z'Z' \to AA(21\%)$	BP4	$Z'Z' \to H^+H^-(46\%)$ $Z'Z' \to h_1h_1(29\%)$ $Z'Z' \to AA(23\%)$
BP5	$Z'Z' \to h_2h_2(97\%)$ $Z'Z' \to H^+H^-(2\%)$		

Natural SUSY: searches for light Higgsinos

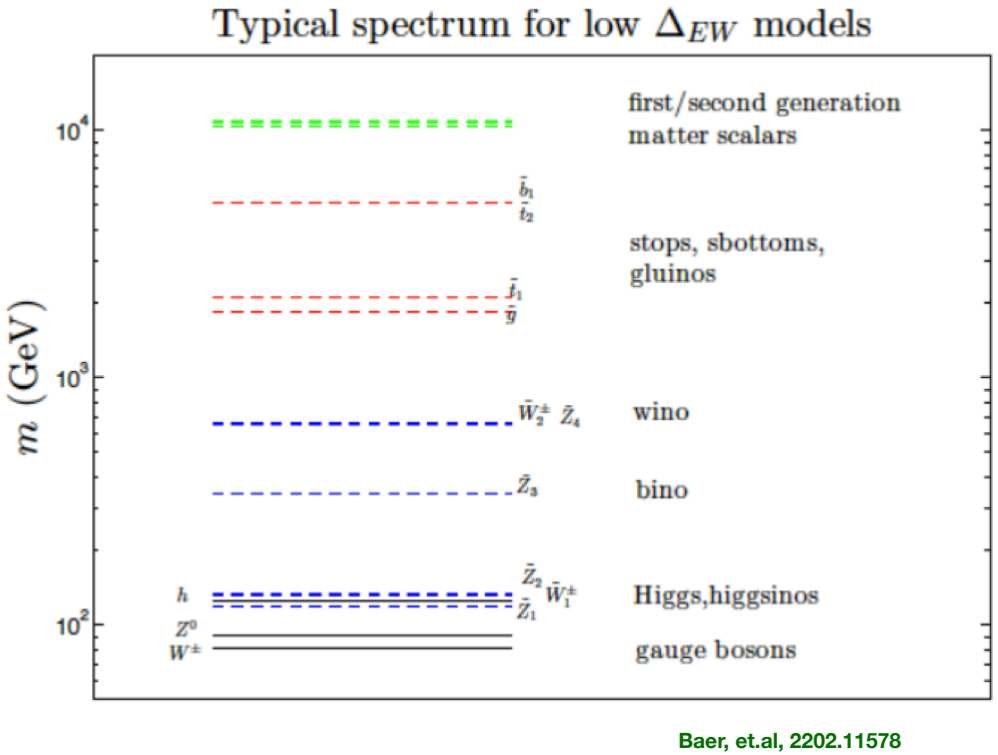

Baer, et.al, 2202.11578

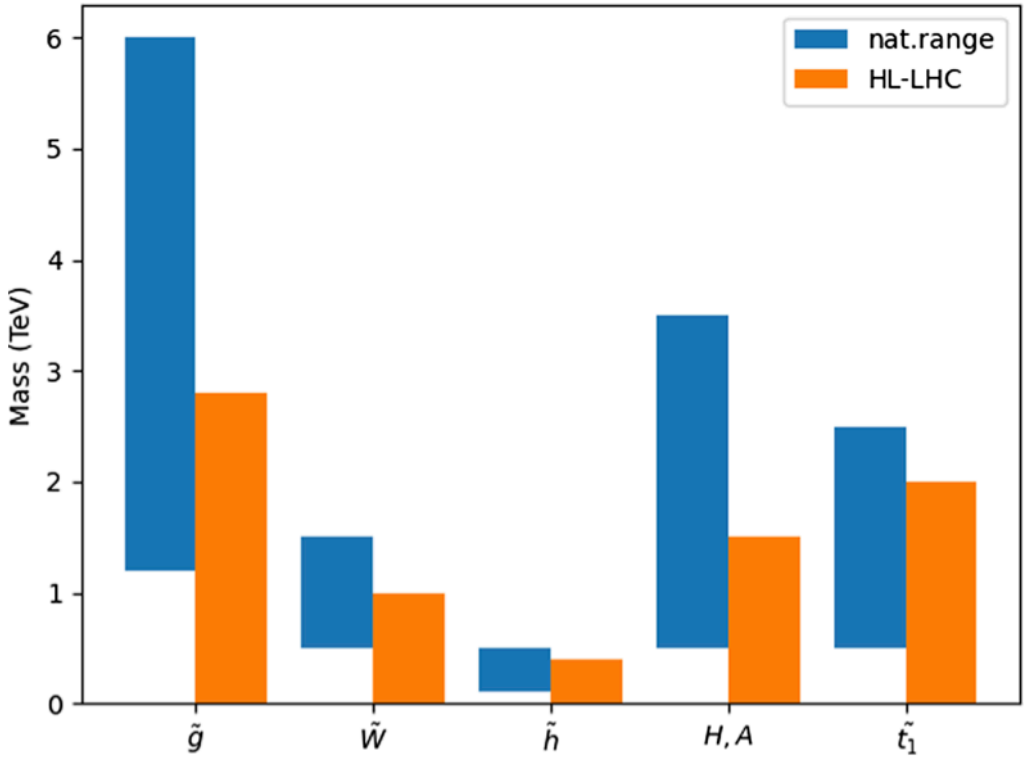

Baer et.al, et.al Rev. Mod. Phys. 97, 045001

Natural SUSY characterized by light Higgsinos still elusive at LHC and natural range of Higgsino masses not expected to be ruled out by end of HL-LHC. LCs better prospects at seeing light Higgsinos!

Breggren,et.al EPJC (2013) 73:2660

Expectations from Naturalness measures for SUSY

- Early estimates of naturalness such as by Barbieri-Gudice, $\Delta_{BG} = max_i|\frac{p_i \partial m_Z^2}{m_Z^2 \partial d p_i}|.$
- Stringent upper limits on gluinos and third generation squarks.

p_i **independent soft terms.**

R. Barbieri and G. F. Giudice, Nucl. Phys. B 306 (1988)

- Conservative measures of naturalness: Δ_{EW} , the ratio of the largest term on the right-hand-side of:

$$\frac{m_Z^2}{2} = \frac{m_{H_d}^2 + \Sigma_d^d - (m_{H_u}^2 + \Sigma_u^u)\tan^2\beta)}{\tan^2\beta - 1} - \mu^2$$

$$\Delta_{EW} = \frac{max|RHS|}{m_Z^2/2}$$

Limits on particles for 3% Δ_{BG} ($\Delta_{BG} < 30$) fine-tuning and for $\Delta_{EW} < 30$.

Mass	BG/DG	Δ_{EW}
μ	<350 GeV	<350 GeV
$m_{\tilde{g}}$	$<400-600$ GeV	<6 TeV
$m_{\tilde{t}_1}$	<450 GeV	<3 TeV
$m_{\tilde{q},\tilde{\ell}}$	$<550-700$ GeV	$<10-30$ TeV

Baer, et.al, 2202.11578

A ~95 GeV excess

Phys.Lett.B565:61-75,2003

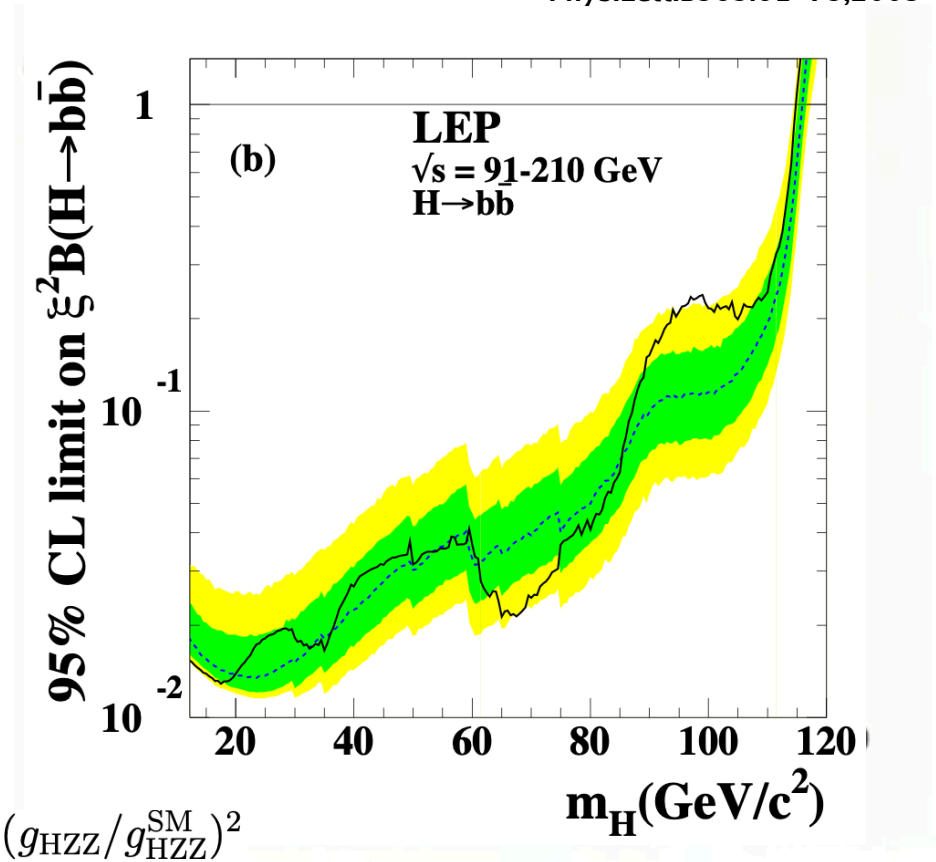

$\xi^2 = (g_{\mathrm{HZZ}}/g^{\mathrm{SM}}_{\mathrm{HZZ}})^2$

~2 σ excess in $b\bar{b}$ mode around 95 GeV

$\mu^{b\bar{b}}_{\mathrm{LEP}} = 0.117^{+0.057}_{-0.057},$

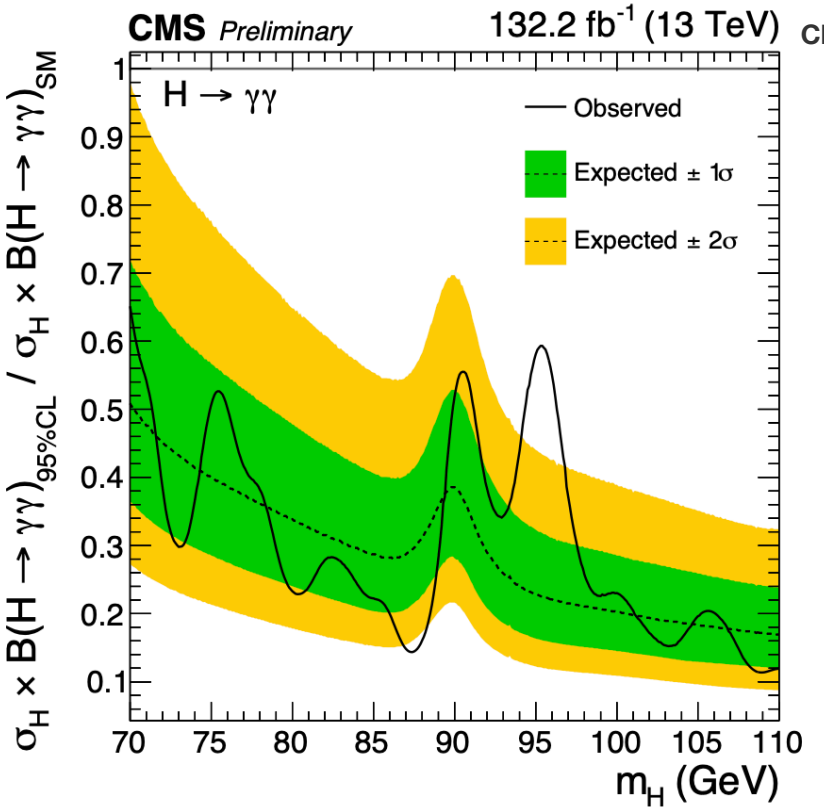

CMS-PAS-HIG-20-002

$\mu^{\mathrm{CMS}}_{\gamma\gamma} = \dfrac{\sigma^{\mathrm{exp}}\,(pp \to \phi \to \gamma\gamma)}{\sigma^{\mathrm{SM}}\,(pp \to H \to \gamma\gamma)} = 0.33^{+0.19}_{-0.12}$

~2.9 σ excess in $\gamma\gamma$ mode,

95 GeV signal strengths

$$\mu^{b\bar{b}}_{\rm LEP} = 0.117^{+0.057}_{-0.057}, \qquad \mu^{\gamma\gamma}_{\rm LHC-combined} = 0.24^{+0.09}_{-0.08},$$

$$\mu^{\rm the}_{\rm LEP} = \frac{\sigma_{\rm 2HDMS}(e^+e^- \to Zh_1)}{\sigma_{\rm SM}(e^+e^- \to ZH^0_{\rm SM})} \times \frac{{\rm BR}_{\rm 2HDMS}(h_1 \to b\bar{b})}{{\rm BR}_{\rm SM}(H^0_{\rm SM} \to b\bar{b})} = |c_{h_1VV}|^2 \frac{{\rm BR}_{\rm 2HDMS}(h_1 \to b\bar{b})}{{\rm BR}_{\rm SM}(H^0_{\rm SM} \to b\bar{b})}$$

$$\mu^{\rm the}_{\rm CMS} = \frac{\sigma_{\rm 2HDMS}(gg \to h_1)}{\sigma_{\rm SM}(gg \to H^0_{\rm SM})} \times \frac{{\rm BR}_{\rm 2HDMS}(h_1 \to \gamma\gamma)}{{\rm BR}_{\rm SM}(H^0_{\rm SM} \to \gamma\gamma)} = |c_{h_1tt}|^2 \frac{{\rm BR}_{\rm 2HDMS}(h_1 \to \gamma\gamma)}{{\rm BR}_{\rm SM}(H^0_{\rm SM} \to \gamma\gamma)}$$

$$\chi^2_{\text{CMS-LEP}} = \left(\frac{\mu^{\rm the}_{\rm LEP} - 0.117}{0.057}\right)^2 + \left(\frac{\mu^{\rm the}_{\rm CMS} - 0.6}{0.2}\right)^2$$

$$c_{h_1tt} = \frac{\sin\alpha_1 \cos\alpha_2}{\sin\beta}, \qquad c_{h_1bb} = \frac{\cos\alpha_1 \cos\alpha_2}{\cos\beta}, \qquad c_{h_1VV} = \cos\alpha_2 \cos(\beta - \alpha_1)\ .$$

S.Heinemeyer et.al,
Phys. Rev. D 106 (2022), no. 7 075003

Interplay of DM and 95 GeV Higgs

m_{h_1}	m_{h_2}	m_{h_3}	m_A	m_{A_S}
95 GeV	125.09 GeV	900 GeV	900 GeV	325.86 GeV
$m_{H^\pm}$	$m_S'^2$	δ'_{14}	δ'_{25}	$\tan(\beta)$
900 GeV	$-4.809 \times 10^4\,\mathrm{GeV}^2$	-9.6958	0.2475	10
v_S	c_{h_1bb}	c_{h_1tt}	$alignm$	$\tilde{\mu}^2$
239.86 GeV	0.2096	0.4192	0.9998	$8.128 \times 10^5\,\mathrm{GeV}^2$

Benchmark point **BP1**

Parameters	Range
c_{h_1bb}	$[0.0996, 0.320]$
c_{h_1tt}	$[0.309, 0.529]$

Parameter ranges for the couplings to fit the 95 GeV excess.

S.Heinemeyer et.al,
Phys. Rev. D 106 (2022), no. 7 075003

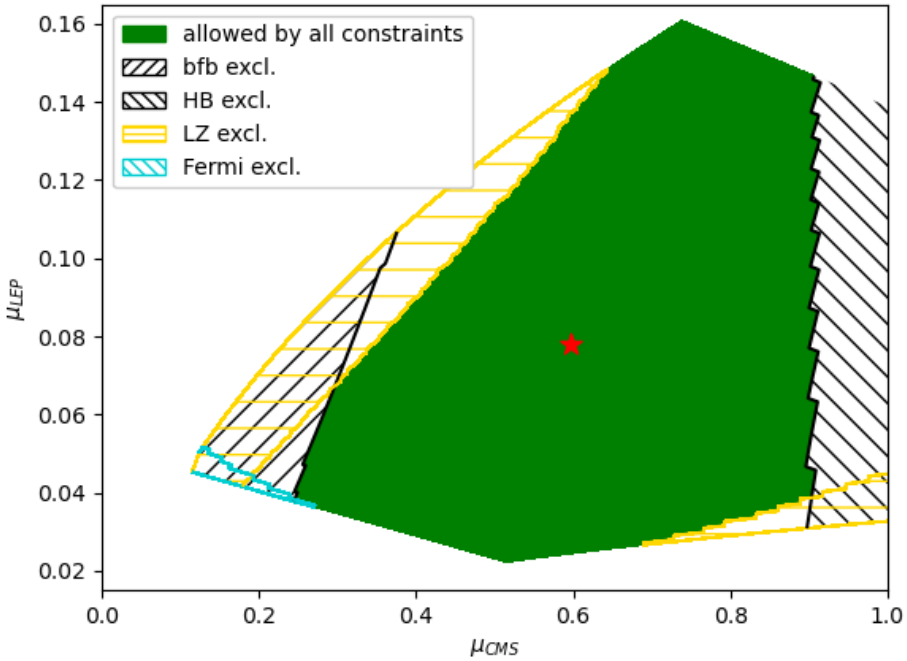

Allowed region consistent with 95 GeV excess, theoretical and experimental constraints from Higgs and dark matter searches.

Dutta, et.al, Eur.Phys.J.Plus 140 (2025) 1, 87

Salient Features from DM observables

- Cancellations between contributions from h_1 and h_2 (blue line).
- Dominant DM annihilation from Di-higgs,WW and bb channels.
- DM relic density mostly under abundant over the scanned parameter space.

Conservative limits placed from LZ and FERMI-LAT.

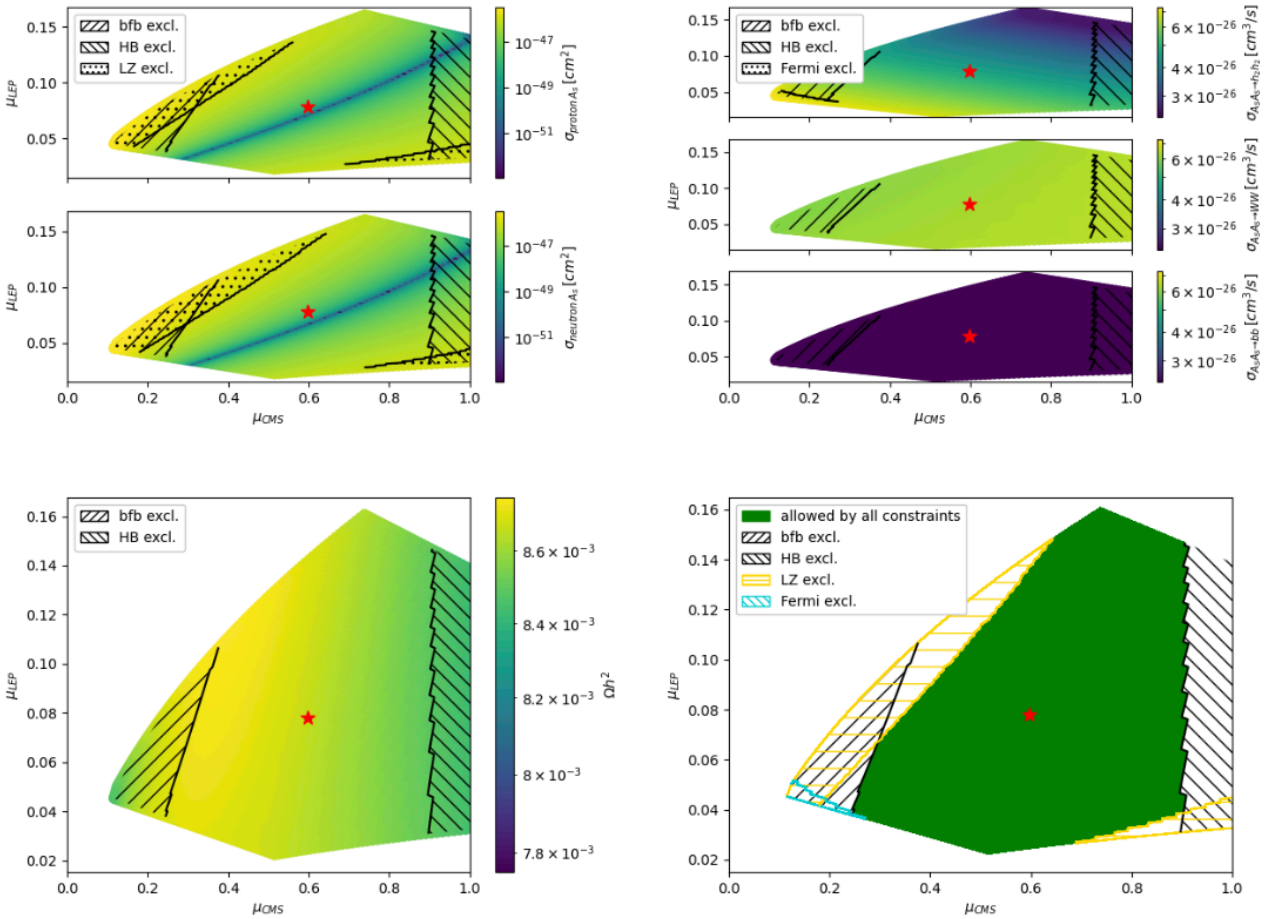

Dutta, et.al, Eur.Phys.J.Plus 140 (2025) 1, 87

Constraints on $\delta'_{14} - \delta'_{25}$

$$\delta'_{14} = \lambda'_4 - \lambda'_1,$$
$$\delta'_{25} = \lambda'_5 - \lambda'_2.$$

- Stringent constraints from LZ and Fermi-LAT data as well from boundedness-from-below constraints.

$$\frac{\lambda_{h_j A_S A_S}}{v} = [\frac{\sum_{i=1}^{3} m_{h_i}^2 R_{i1} R_{i3}}{3vv_S \cos(\beta)} + \frac{4\delta'_{14}}{3}]c_\beta R_{j1}$$
$$+ [\frac{\sum_{i=1}^{3} m_{h_i}^2 R_{i2} R_{i3}}{3vv_S \sin(\beta)} + \frac{4\delta'_{25}}{3}]s_\beta R_{j2}$$
$$- [\frac{2}{vv_S}(2m'^2_S + m^2_{A_S} + (\frac{\sum_{i=1}^{3} m_{h_i}^2 R_{i1} R_{i3}}{3vv_S \cos(\beta)} + \frac{\delta'_{14}}{3})2v^2 c^2_\beta$$
$$+ (\frac{\sum_{i=1}^{3} m_{h_i}^2 R_{i2} R_{i3}}{3vv_S \sin(\beta)} + \frac{\delta'_{25}}{3})2v^2 s^2_\beta) + \frac{\sum_{i=1}^{3} m_i^2 R^2_{i3}}{vv_S}]R_{j3},$$

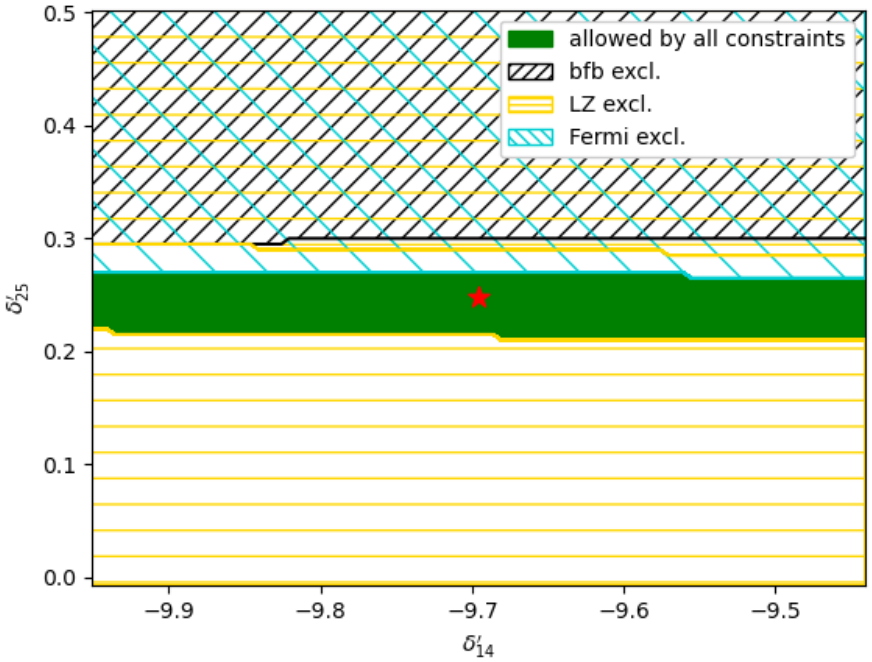

Allowed by all constraints.

Effect of δ'_{25} dominant δ'_{14} over due to multiplicative factor of $\sin\beta$.

- $\delta'_{25} \simeq 0.25$ to satisfy constraints from LZ => allowed region from cancellations between h_1 and h_2.

Dutta, et.al, Eur.Phys.J.Plus 140 (2025) 1, 87

Minimization Equations

$$
\begin{aligned}
m_{11}^2 v_1 - m_{12}^2 v_2 + \frac{\lambda_1}{2} v_1^3 + \frac{\lambda_{345}}{2} v_1 v_2^2 + (\frac{\lambda_1'}{2} v_1 + \lambda_4' v_1) v_S^2 = 0, \\
m_{22}^2 v_2 - m_{12}^2 v_1 + \frac{\lambda_2}{2} v_2^3 + \frac{\lambda_{345}}{2} v_1^2 v_2 + (\frac{\lambda_2'}{2} v_2 + \lambda_5' v_2) v_S^2 = 0, \\
m_S^2 v_S + m_S'^2 v_S + \frac{\lambda_1''}{12} v_S^3 + \frac{\lambda_2''}{3} v_S^3 + \frac{\lambda_3''}{4} v_S^3 + \frac{v_S}{2}(\lambda_1' v_1^2 + \lambda_2' v_2^2) + \\
v_S(\lambda_4' v_1^2 + \lambda_5' v_2^2) = 0.
\end{aligned}
$$

Scalar mass matrix

$$
M_S^2 = \begin{pmatrix}
m_{12}^2 \frac{v_2}{v_1} + \lambda_1 v_1^2 & -m_{12}^2 + \lambda_{345} v_1 v_2 & (\lambda_1' + 2\lambda_4') v_1 v_S \\
-m_{12}^2 + \lambda_{345} v_1 v_2 & m_{12}^2 \frac{v_1}{v_2} + \lambda_2 v_2^2 & (\lambda_2' + 2\lambda_5') v_2 v_S \\
(\lambda_1' + 2\lambda_4') v_1 v_S & (\lambda_2' + 2\lambda_5') v_2 v_S & (\frac{5\lambda_1''}{6} + \frac{\lambda_3''}{2}) v_S^2
\end{pmatrix}
$$

Dutta, *et.al, Eur.Phys.J.Plus 140 (2025) 1, 87*

Boundedness-From-Below conditions

in the basis $X = \left(\Phi_1^\dagger\Phi_1,\ \Phi_2^\dagger\Phi_2,\ \rho_S^2,\ \eta_S^2\right)^T$, with $S = \rho_S + i\eta_S$:

$$min[V_4] = X^T \frac{1}{2} \underbrace{\begin{pmatrix} \lambda_1 & \lambda_3 + \rho^2(\lambda_4 - |\lambda_5|) & \lambda_1' + 2\lambda_4' & \lambda_1' - 2\lambda_4' \\ \lambda_3 + \rho^2(\lambda_4 - |\lambda_5|) & \lambda_2 & \lambda_2' + 2\lambda_5' & \lambda_2' - 2\lambda_5' \\ \lambda_1' + 2\lambda_4' & \lambda_2' + 2\lambda_5' & \frac{5\lambda_1'' + 3\lambda_3''}{6} & \frac{-\lambda_1'' + \lambda_3''}{2} \\ \lambda_1' - 2\lambda_4' & \lambda_2' - 2\lambda_5' & \frac{-\lambda_1'' + \lambda_3''}{2} & \frac{-\lambda_1'' + \lambda_3''}{2} \end{pmatrix}}_{A} X$$

$$= \frac{1}{2} X^T A X, \tag{3.1}$$

where two cases are distinguished:

$$\begin{aligned} &\text{case 1: } (\lambda_4 - |\lambda_5|) \geq 0 \quad \Rightarrow \quad \min[V_4] = V_4|_{\rho=0} \\ &\text{case 2: } (\lambda_4 - |\lambda_5|) < 0 \quad \Rightarrow \quad \min[V_4] = V_4|_{\rho=1}. \end{aligned}$$

Kannike, Eur. Phys. J. C 72, 2093 (2012)

Dutta, *et.al, Eur.Phys.J.Plus 140 (2025) 1, 87*

The explicit copositivity conditions for a symmetric order 3 matrix B with entries b_{ij}, $i, j = 1, 2, 3$ can be found in [53, eq. (5) and (6)] and are:

$$b_{11} \geq 0, \quad b_{22} \geq 0, \quad b_{33} \geq 0, \tag{3.2}$$

$$\bar{b_{12}} = b_{12} + \sqrt{b_{11} b_{22}} \geq 0, \tag{3.3}$$

$$\bar{b_{13}} = b_{13} + \sqrt{b_{11} b_{33}} \geq 0, \tag{3.4}$$

$$\bar{b_{23}} = b_{23} + \sqrt{b_{22} b_{33}} \geq 0, \tag{3.5}$$

$$\sqrt{b_{11} b_{22} b_{33}} + b_{12}\sqrt{b_{33}} + b_{13}\sqrt{b_{22}} + b_{23}\sqrt{b_{11}} + \sqrt{2\bar{b_{12}}\bar{b_{13}}\bar{b_{23}}} \geq 0. \tag{3.6}$$

The matrix A has to satisfy: $\det(A) \geq 0 \quad \vee \quad (\mathrm{adj}A)_{ij} < 0$, for some i, j. The adjugate of A is defined as the transpose of the cofactor matrix: $(\mathrm{adj}A)_{ij} = (-1)^{i+j} D_{ji}$, with D_{ij} being the determinant of the submatrix that is obtained by deleting the i-th row and j-th column from A.

Weakly Interacting Massive Particles (WIMPs)

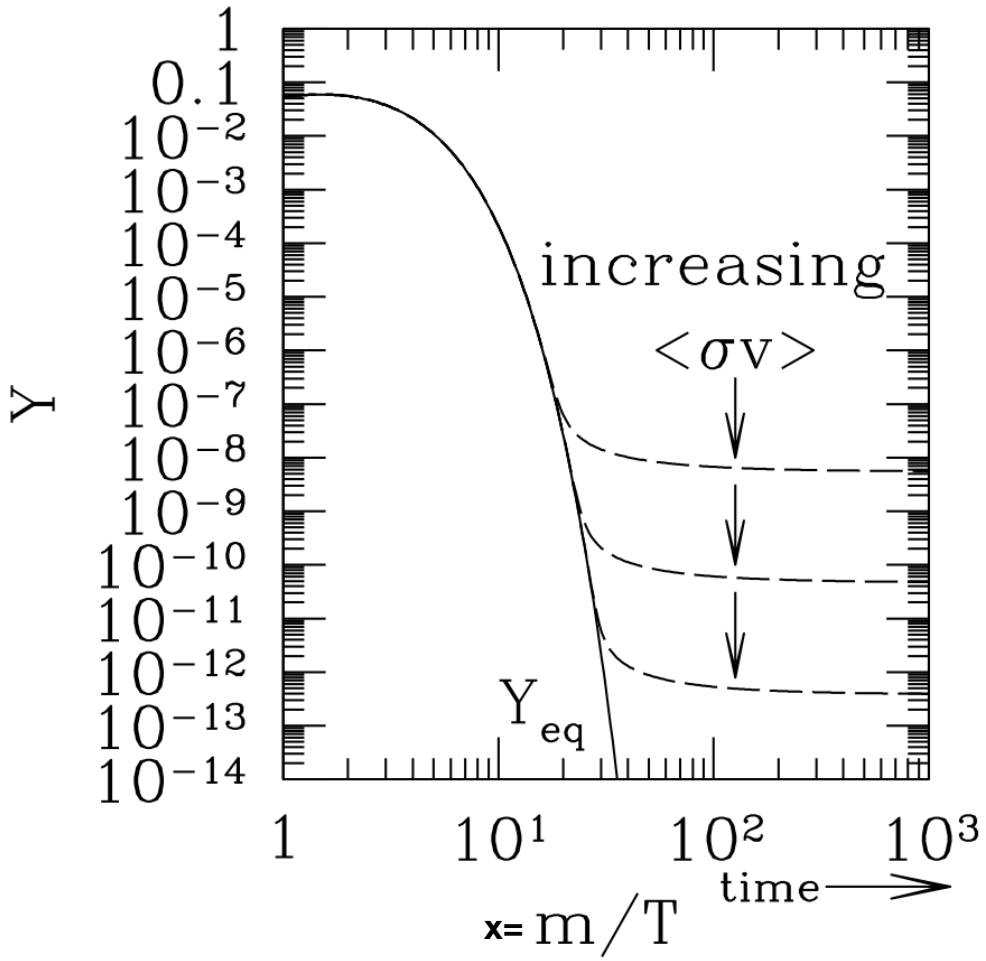

- The Boltzmann Transport equation:

$$\frac{dY}{dx} = \frac{1}{3H}\frac{ds}{dx}\langle\sigma_A v\rangle\left(Y^2 - Y_{EQ}^2\right).$$

$$\Omega h^2 \approx \frac{3\times 10^{-27}\ \mathrm{cm}^3/\mathrm{s}}{\langle\sigma_{\mathrm{ann}} v\rangle}$$

E. W. Kolb and M. S. Turner, Front. Phys. 69, 1 (1990).

Constraints on DM from Direct Detection

Spin-Independent DM-nucleon cross-section.

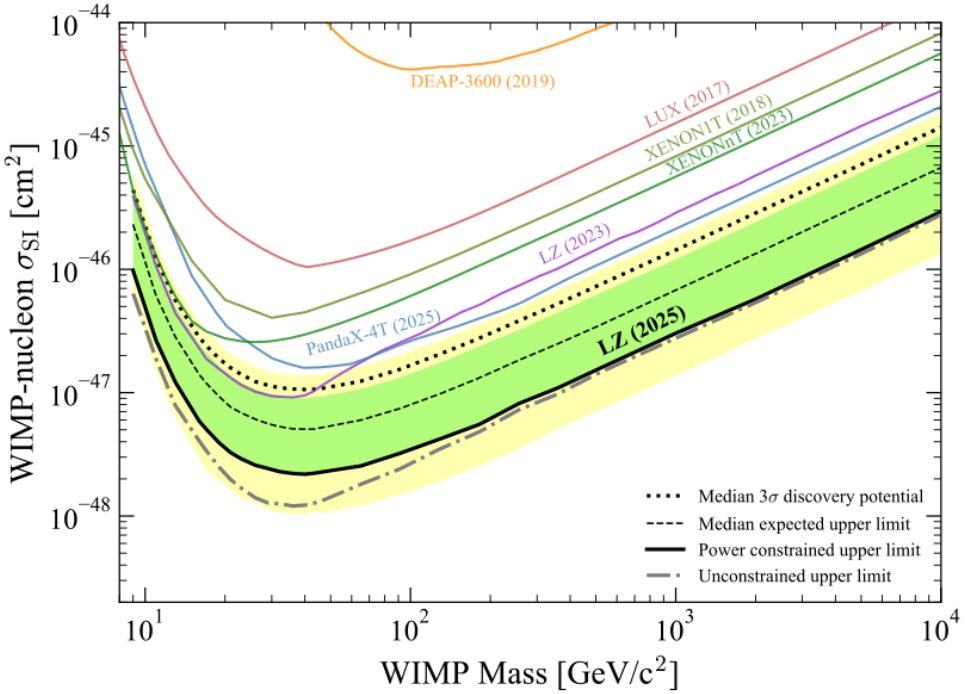

Spin-Dependent DM-nucleon cross-section.

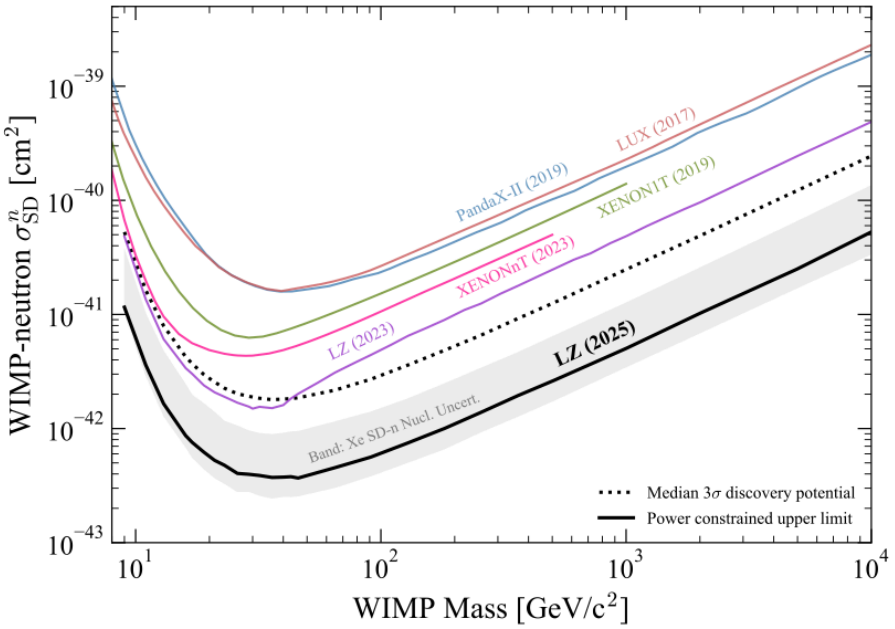

LZ Collaboration, Phys. Rev. Lett. 135,011802

Indirect Detection

- Combined upper limits on annihilation cross-section from Fermi-LAT on bb and $\tau\tau$ modes.

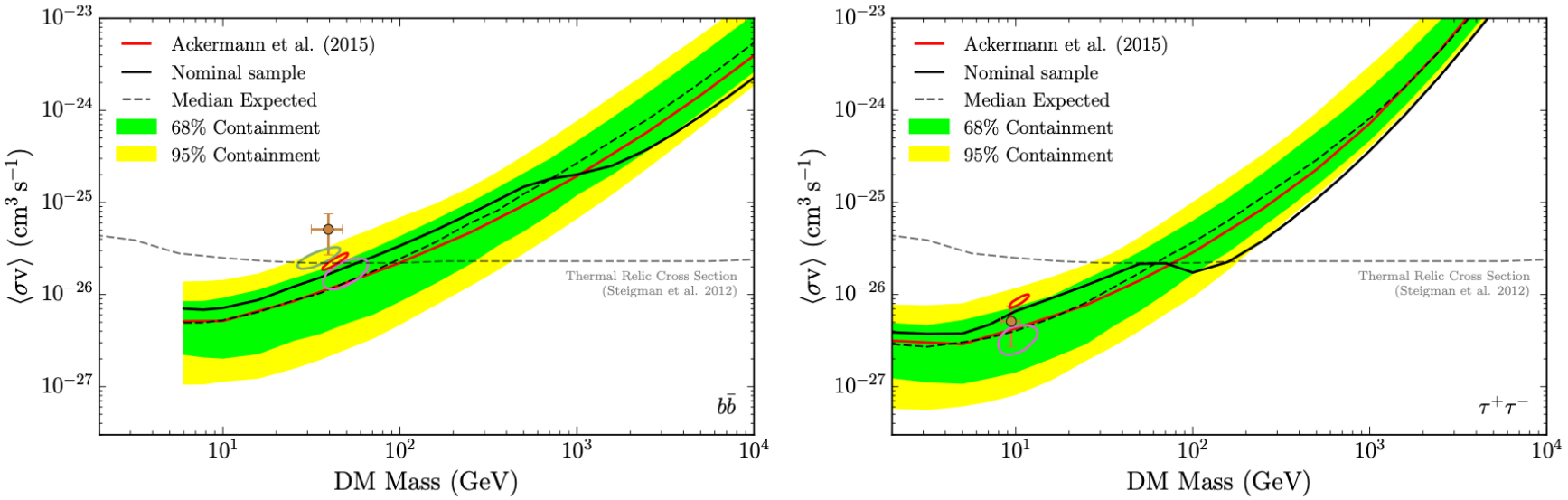

Fermi-LAT. Astrophys. J. 834(2), 110 (2017)